

5

Ordered Mesoporous Silica

5.1 MCM-41 and MCM-48 – Revolution by the Mobil Oil Company

5.1.1 The Original Papers and Patents

Zeolites and zeotypes, combined with the mesoporous amorphous silica and alumina were, and are still, the materials of choice in bulk chemistry and the petrochemical industry. They are cheap and robust and the entire industry has built large production facilities based on these porous catalysts and supports, so it is not obvious to introduce alternatives. But the small pore sizes of zeolites stimulated researchers to keep on searching for materials with larger pores.

So, it was an oil company, the then-called Mobil Oil Company (currently merged into Exxon Mobil) that patented and published the very first report on a “templated mesoporous silica” with uniform mesoporous pores in 1992 [1].

Actually, ordered mesoporous materials were reported for the first time in 1990 by Kuroda and coworkers [2]. A hydrothermal synthesis was described where sodium ions in the interlayer space of Kanemite are exchanged with alkyltrimethylammonium chloride ions. By increasing the alkyl chain in the alkyltrimethylammonium ions, mesopores between 2 and 4 nm and surface areas of about $900 \text{ m}^2 \text{ g}^{-1}$ were attained. In a subsequent report by Inagaki et al. [3], optimization of the reaction conditions led to a highly ordered mesoporous material with a hexagonal unit cell. The hexagonal honeycomb structure was clearly visible by Transmission Electron Microscopy (TEM). However, in the meantime the Mobil Research and Development Corporation reported their breakthrough research on a new family of ordered mesoporous materials, designated M41S [1b, c]. Most likely inspired by the development of large pore crystalline materials like zeotype VPI-5, Kresge et al. prepared mesoporous silicas with both hexagonal (MCM-41) and cubic (MCM-48) symmetry with pore sizes ranging between 2 and 10 nm, by employing surfactants. After the first patents on these materials appeared [1b, 4], a publication in *Nature* [1c] and one in the *Journal of the American Chemical Society (JACS)* [1b] followed. With over 12 000 citations (1992–2008), these two papers form the foundation of the field of ordered mesoporous materials.



Wieslaw J. Roth (left) and Charles T. Kresge (right) were two of the many authors of the Nature paper in 1992. Roth retired from ExxonMobil in 2009 and is now a professor in Krakow (Poland). Charles (Charlie) Kresge became R&D Vice President of the Dow Chemical Company after he left the Mobil Oil Company in 1999. These authors and many others of the Nature paper received several prizes and medals for their groundbreaking work

(Photograph taken from ref. [5]).

The idea was simply genius, briefly: dissolve a surfactant in an acid or basic solution at such conditions that it form micelles, “liquid crystals.” This is obtained at the so-called Critical Micelle Concentrations (CMC). The first CMC (CMC-1) is the concentration at which spherical micelles are observed. The second CMC (CMC-2) is the concentration at which spherical micelles start to transform into rodlike micelles ([Figure 5.1](#)). The values are largely dependent on the type of surfactant, but also on the synthesis conditions. For instance, with increasing temperature, the required concentration of surfactants for a sphere-to-rod transformation to occur increases.

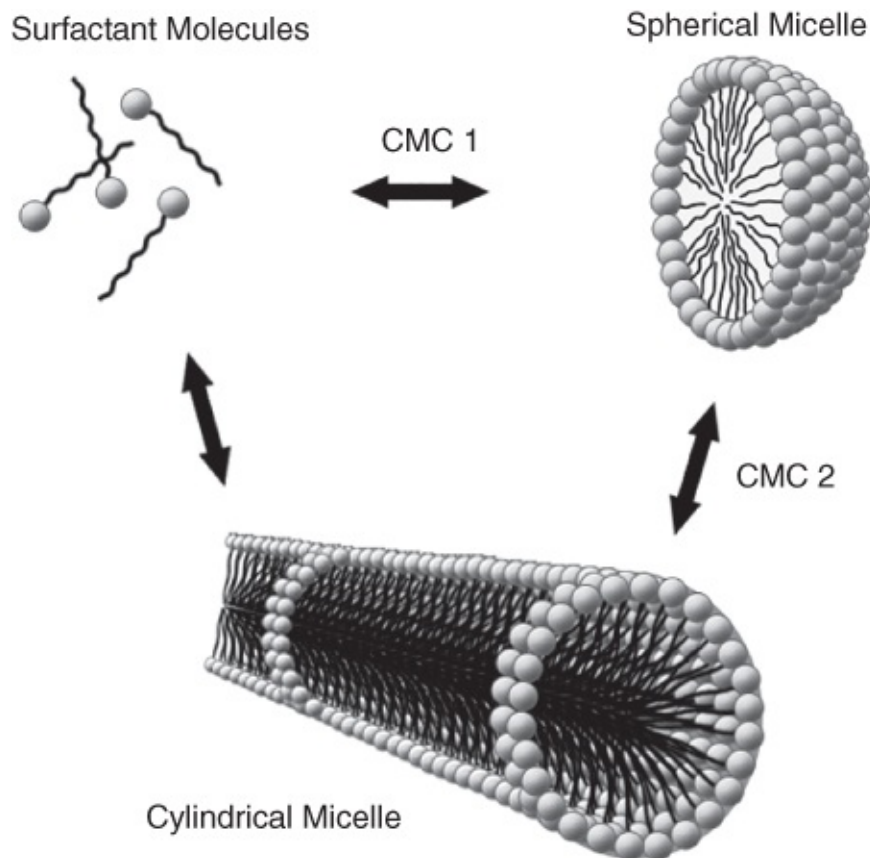


[Figure 5.1](#) Dynamic equilibria in a surfactant-water system.

Now, introduce a hydrolysable silica source (typically tetraethoxysilane [TEOS], $\text{Si}(\text{OEt})_4$) to this surfactant solution and the silica will grow and form uniform pores around the surfactant (see [Chapter 4](#)). During synthesis, long-chained organic cationic surfactants are used to assemble silicate anions from solution until the formation of a dense Si-network around the micelles. A final calcination removes the organics and leads to highly porous solids with pores ≥ 2 nm and surface areas reaching $1000 \text{ m}^2 \text{ g}^{-1}$. This is shown as Mechanism 1 in [Figure 5.2](#).

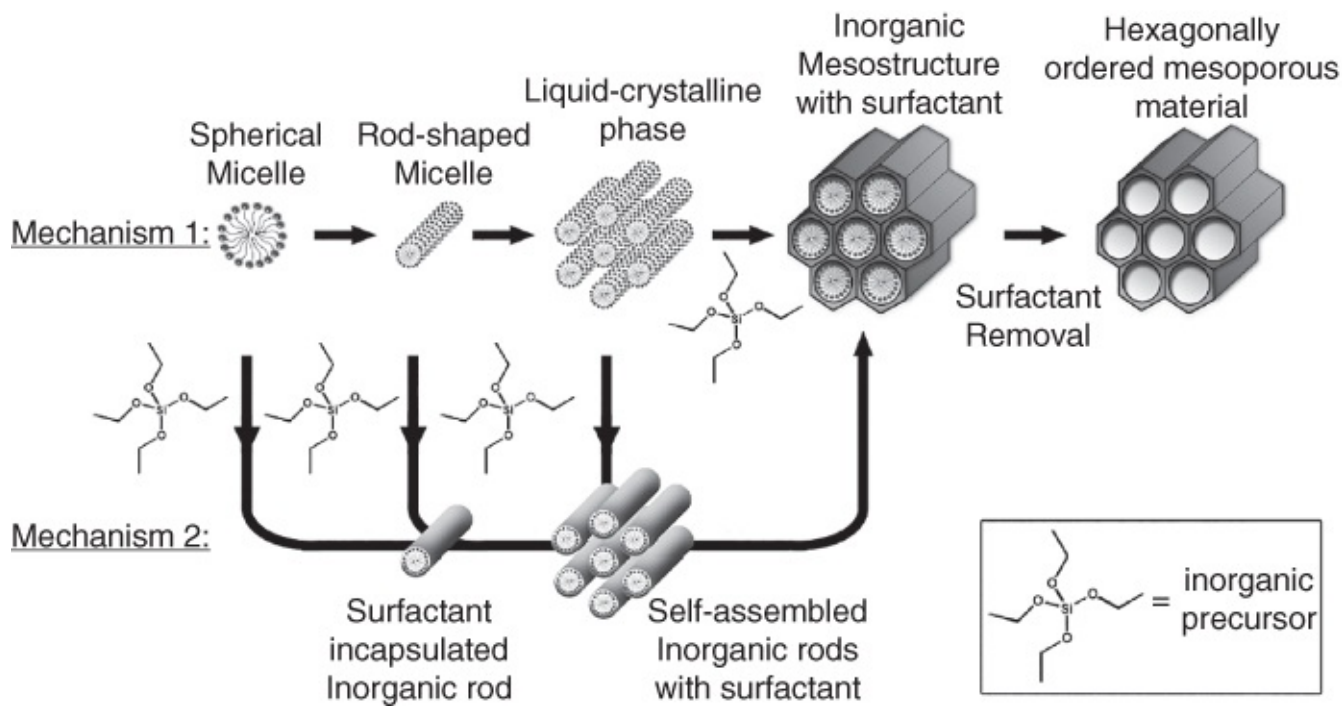


Figure 5.2 Possible mechanisms involved in mesostructure formation. Path 1 is the true liquid-crystal templating mechanism, Path 2 is designated as the cooperative liquid-crystal mechanism.

Source: Reproduced with permission of ACS. Adapted from [1b].

The general class of materials was named M41S and more than 20 examples were presented, using different synthesis conditions, yielding a hexagonal, one-dimensional phase (MCM-41), a cubic, three-dimensional phase (MCM-48) or a two-dimensional lamellar phase (MCM-50). There is some confusion about the nature of the abbreviation MCM; some say it means Mobil Catalytic Materials, others that it means Mobil Composition of Matter.

Figure 5.3 shows an artistic drawing of the different MCM structures. The three major forms are MCM-41, a hexagonally ordered silica material; it has the space group $P6mm$. MCM-48 is a cubically ordered silica: the light material is the silica, the two darker rods are the surfactants, they are intertwined, forming a cubic structure in the space group $Ia\bar{3}d$. A third form is a lamellar silica structure, with layers of silica, a bit like a phyllosilicate clay. The typical wall thickness of these original MCM materials was around 1 nm, the pore size varied depending on the surfactant and synthesis conditions around a 2–4 nm diameter.

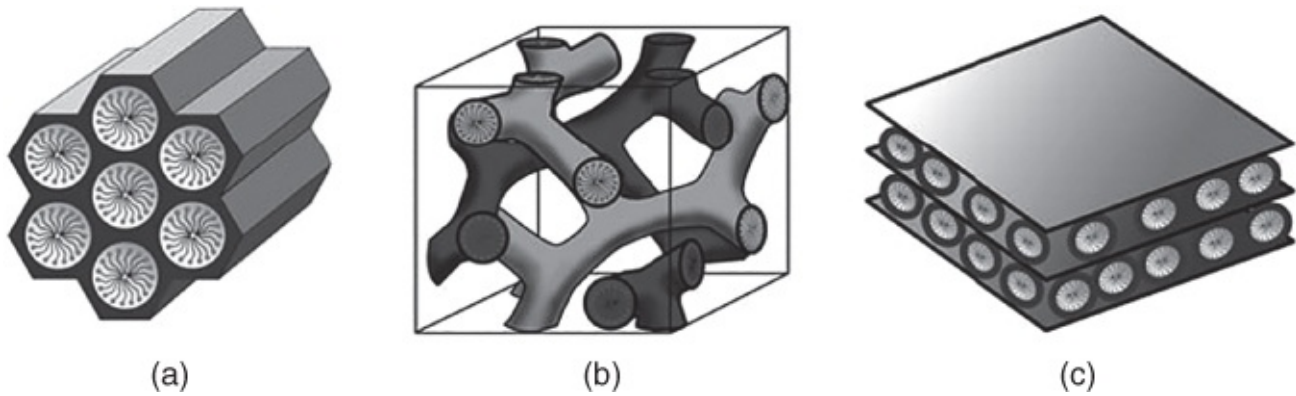


Figure 5.3 The three phases: (a) hexagonal MCM-41, (b) cubic MCM-48, (c) lamellar MCM-50.

Source: Reproduced with permission of John Wiley & Sons, Ltd. Adapted from [6].

The hexagonal ordering of the MCM-41 materials was clearly visible in electron microscopy. In [Figure 5.4](#), we show the original TEM image of the MCM-41 as published by the inventors. The hexagonal ordering (honeycomb ordering) of the materials is clearly visible and the uniformity of the pores is also evident.

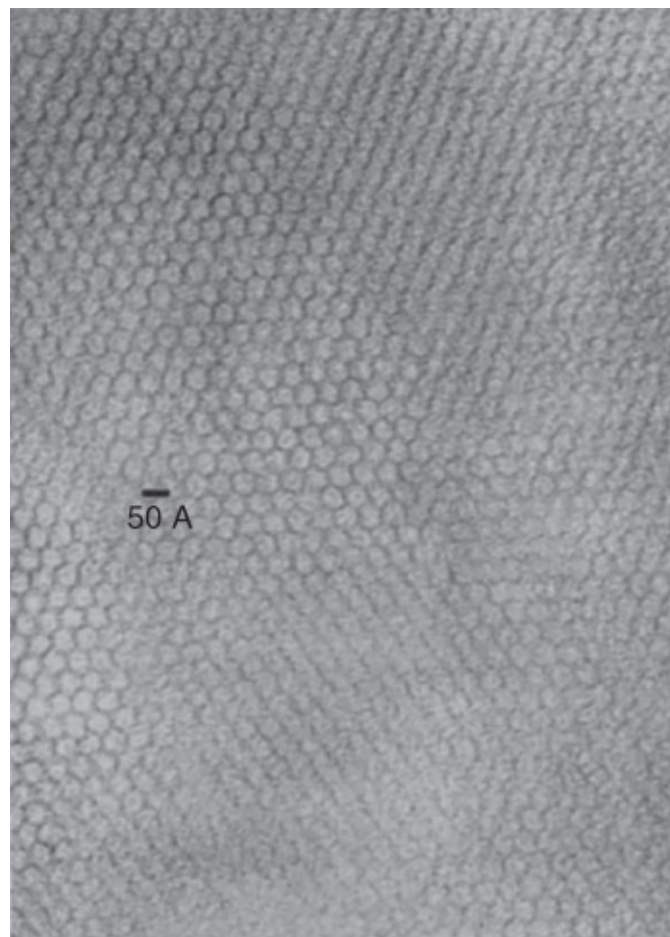
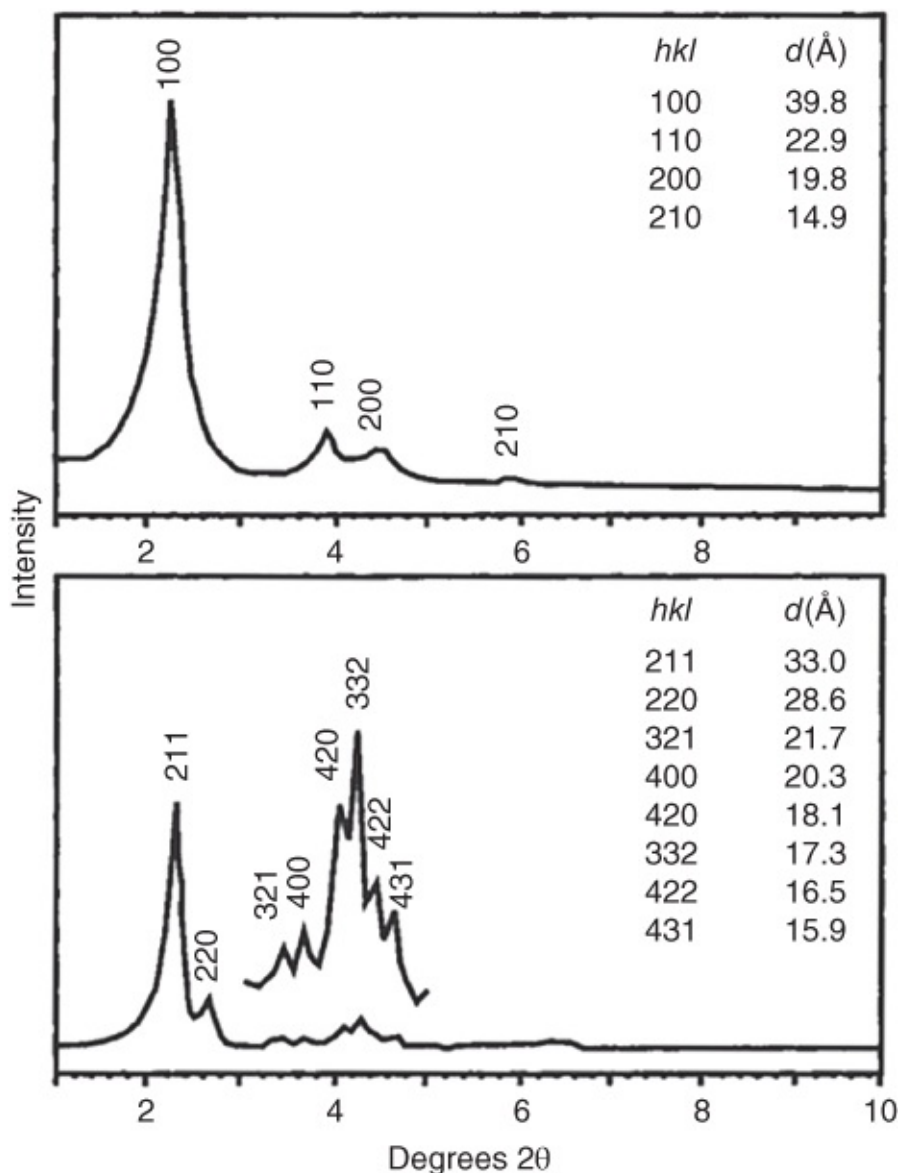


Figure 5.4 Original TEM image of the first report on MCM-41.

Source: Reproduced with permission of Springer Nature [1c].

Another indispensable technique in the characterization of these materials is powder X-Ray

Diffraction (XRD). The simple hexagonal honeycomb structure of MCM-41 is a typical example. The XRD patterns of these materials (see [Figure 5.5](#)), show only the reflections of the honeycomb ordering of the pores, such long-distance reflection peaks are therefore typically at very low angles. The XRD patterns do not show any sign of atomic ordering, the silica walls themselves are amorphous, in contrast to all zeolites and zeotypes discussed earlier. Sometimes these materials are thus referred to as “semi-crystalline”: the pores are ordered, but the atoms creating the walls are not ordered. The ordering of the pores is referred to as mesoscopic ordering: ordering at the meso-scale.



[Figure 5.5](#) XRD patterns of MCM-41 and MCM-48.

Source: Reproduced with permission of ACS [\[1b\]](#).

Similar observations are seen for the (more complex) $Ia\bar{3}d$ structure of MCM-48.

The Mobil Oil researchers discovered a third phase, a lamellar phase, denoted MCM-50. This phase received less attention as it has little potential for applications, but it is an important phase to understand and rationalize the formation mechanism of, as we will do in subsequent

sections.

Another matter that still remains a topic of interest is the manner in which the micelles aggregate into a liquid-crystal. At the time, the researchers of Mobil proposed two synthesis mechanisms to explain the formation of M41S type materials [1b, c]. These two mechanisms are illustrated in Figure 5.2. In the first mechanism, the surfactant liquid-crystal phase is formed prior to the addition of the inorganic species and directs the growth of the inorganic mesostructures. However, this mechanism did not meet much support in the literature [7]. In 1995, Cheng et al. pointed out that the liquid-crystal phase in a CTAC-water (cetyltrimethylammonium chloride) system only forms when the concentration of CTAC is higher than 40 wt% [7b]. CTAC is cetyl trimethyl ammonium chloride, the surfactant used by the Mobil researchers in their first reports; the bromide form is also often used (cetyltrimethylammonium bromide [CTAB]). In the conventional synthesis procedure of MCM-41, the CTAC concentration is much lower than 40 wt%, and only micelles can exist in solution. Because MCM-41 could be formed at surfactant concentrations as low as 1 wt%, it was very doubtful that this first mechanism occurred [7a].

In the second mechanism proposed by the researchers at Mobil, the presence of an inorganic species in the synthesis mixture initiates the formation of the liquid-crystal phase and facilitates the formation of inorganic mesostructures [1b, c]. Under the reaction conditions described by the researchers of Mobil, this mechanism is more realistic and therefore has encountered more acceptance in the literature [7b]. It is called the cooperative mechanism.

Davis and coworkers [7a] found that randomly distributed rod-shaped surfactant micelles form initially and as such interact with inorganic oligomers to form randomly oriented surfactant encapsulated inorganic rods. Upon heating, a base-catalyzed condensation between inorganic species on adjacent rods occurs. This condensation initiates long-range hexagonal ordering, which corresponds to the minimum energy configuration for the packing of the rods.

5.1.2 Calculating the Wall Thickness

Based on both the X-Ray Diffractograms (Chapter 3) and the nitrogen sorption (Chapter 2) isotherms, the pore wall thickness of the materials can be calculated.

In the example of MCM-41 hexagonal structure, the d_{100} spacing can be calculated using the Bragg equation (Chapter 3). The d -spacing is the distance between the centers of the pores of two layers, whereas the lattice parameter a_0 represents the distance between the centers of two adjacent pores. This is shown in Figure 5.6, where we have drawn the pores further apart for reasons of clarity. The relationship between the d_{100} distance and the lattice unit cell parameter a_0 for the honeycomb $P6mm$ symmetry is given by the following equation

$$d = \frac{1}{\sqrt{\frac{4(h^2+hk+k^2)2}{3a_0^2} + \frac{l^2}{c^2}}} \quad 5.1$$

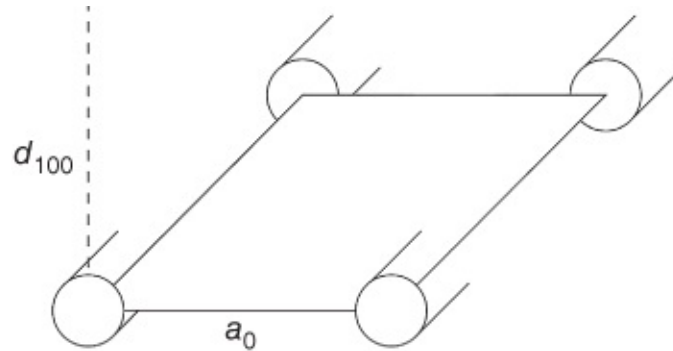


Figure 5.6 Relationship between unit cell and d-spacing in MCM-41.

This equation reduces for a $(hkl) = (100)$ and $c = \infty$ to

$$a_0 = \frac{2}{\sqrt{3}}d_{100} \quad 5.2$$

The pore diameter, D_p , derived directly from the pore analysis by nitrogen or argon sorption can then be used to calculate the wall thickness, t , according to Kruk, Sayari, and Jaroniec [8]:

$$t = a_0 - 0.95D_p \quad 5.3$$

Similar calculations can be made for other morphologies, for all cubic symmetries, the relation between a_0 and d is

$$a_0 = d_{hkl} \cdot \sqrt{h^2 + k^2 + l^2} \quad 5.4$$

For the $Ia\bar{3}d$ cubic structure, the wall thickness can be calculated, by the formula derived by Ravikovitch and Neimark [9]:

$$t = \frac{a_0}{3.0919} - \frac{D_p}{2} \quad 5.5$$

For another cubic geometry, with a $Im\bar{3}m$ space group, seen in for instance the SBA-16 (see later), the relationship is written as

$$t = \frac{\sqrt{3}}{2} a_0 - D_p$$

5.1.3 Interaction Between Surfactant and Inorganic Precursor

The first templates used were ionic surfactants with alkyl chains that are around 16 carbons in length. It was suggested that, in a basic medium, the silicate/silica species that arise from the hydrolysis of TEOS are negatively charged and are then attracted to the positively charged ammonium groups of the cationic surfactant. CTAB is the most often-used surfactant in this type of synthesis. This interaction is visualized in [Figure 5.7](#).

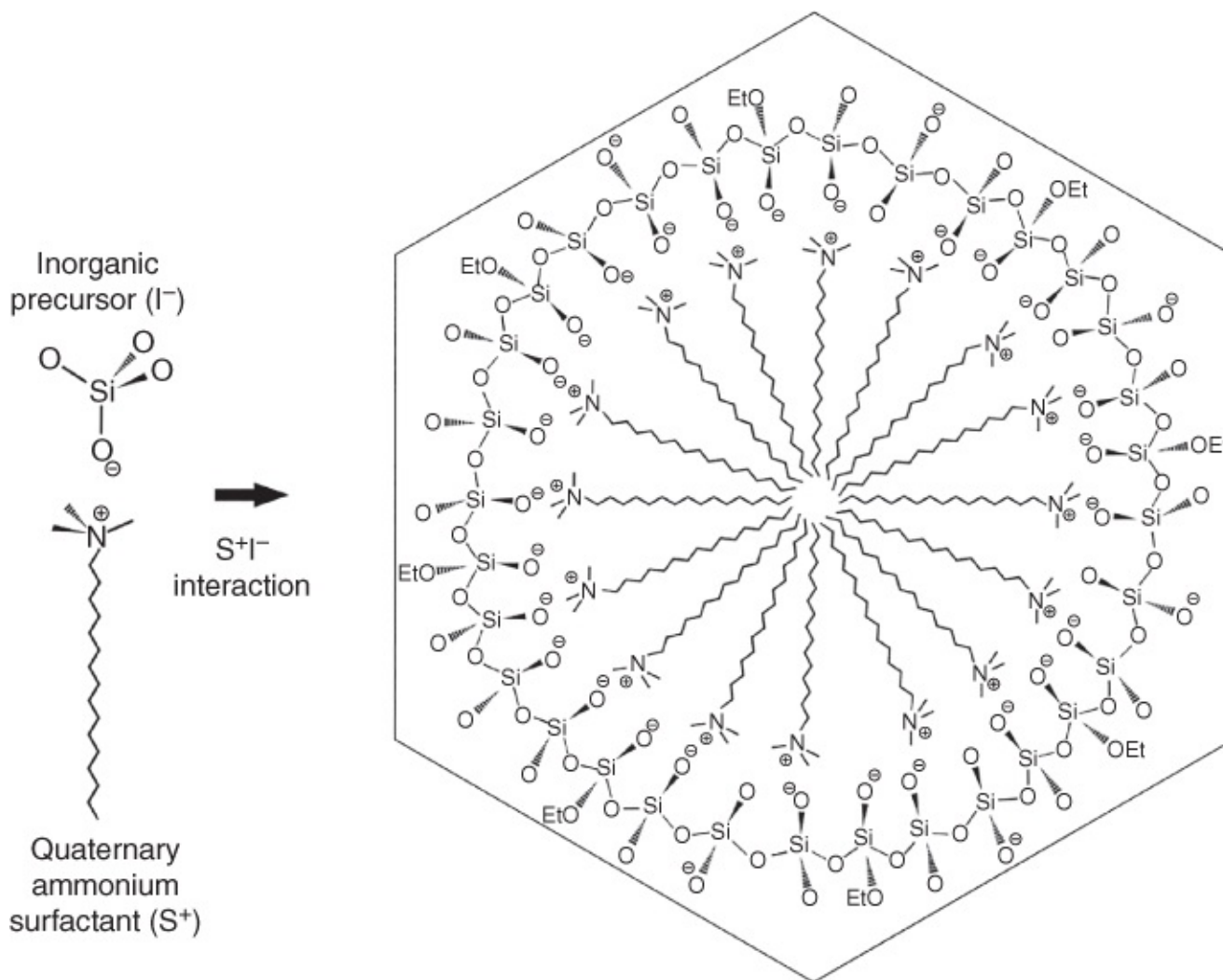


[Figure 5.7](#) S⁺I⁻ interaction during the synthesis of MCM-41 in basic conditions.

Strangely, the synthesis works just as well in acidic media. In this case, the chloride ions from the HCl form an ion bridge between the now positively charged silicate/silica species and the positively charged surfactant.

These types of interactions were described as S⁺I⁻ and S⁺X⁻I⁺, respectively, with S being the surfactant, I the inorganic species and X the bridging ion. Huo et al. [10] were the first to draw a general mechanism for the interaction between the inorganic precursor (I) and the

surfactant (S).

The inorganic precursor should be capable of forming flexible polyionic species and should undergo extensive polymerization. Furthermore, charge density matching between the surfactant and the inorganic species should be possible. Based on these concepts, four different categories of surfactant-precursor interactions were proposed, as illustrated in [Figure 5.8\(a–d\)](#). The first category (a) involves the charge density matching between cationic surfactants and anionic inorganic species (S^+I^-). Considering the conventional basic (pH > 10) synthesis procedure described by the researchers of Mobil, the inorganic precursor is anionic (I^-), while the surfactant is a cationic quaternary ammonium ion (S^+).

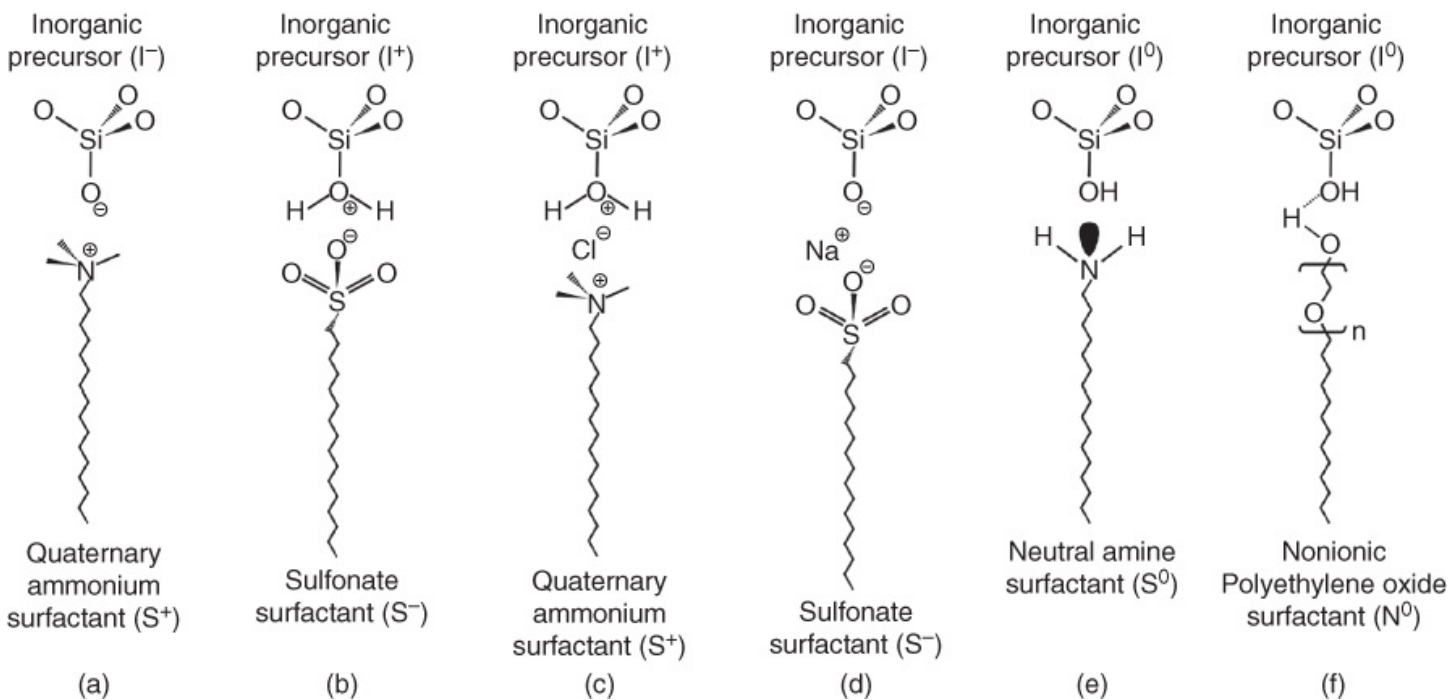


Figure 5.8 Interactions between surfactants and silica.

The second category (b) involves the charge density matching between anionic surfactants and cationic inorganic species (S^-I^+) Huo et al. reported both the synthesis of iron and lead oxide mesoporous materials using anionic sulfonate surfactants [10]. The third (c) and fourth (d) categories are counterion-mediated interactions that allow the assembly of cationic or anionic inorganic species via halide ($S^+X^-I^+$) or alkali metal ($S^-M^+I^-$) ions, respectively.

This way, the synthesis of M41S type materials is feasible both under basic and acidic conditions. By operating under acidic conditions below the isoelectric point of silica (pH = 2), the silicate species are cationic (I^+). The same ammonium surfactant (S^+) can be employed as a templating agent, but in this case the halide counteranion (X^-) is involved in the interaction between the silicate species and the surfactant [10]. The halide counteranion serves to buffer the repulsion between the cationic silicate (I^+) and surfactant (S^+) molecules by means of weak hydrogen-bonding forces. On the other hand, negatively charged surfactants such as long-chain alkyl phosphates or sulfonates (S^-), can be used as templates in basic media if the interaction with the negatively charged silica species (I^-) involves a

metal counterion (M^+) [10].

Soon after Huo reported on the generalized liquid-crystal templating mechanism based on electrostatic interactions between inorganic precursors and surfactants, Pinnavaia et al. proposed a fifth category to synthesize inorganic mesoporous materials (Figure 5.8e) [11]. This synthesis involves a neutral templating mechanism based on hydrogen bonding between neutral primary amines and neutral inorganic precursor molecules ($S^{\circ}I^{\circ}$). These materials will be discussed in Section 5.1.5.

Another hydrogen-bonding synthesis method (f), also reported by Pinnavaia et al., involves surfactants with poly(ethylene oxide) head groups [12]. Due to the adjustable length of the surfactant tail and head group, pores in the range of 2.0–5.8 nm could be attained. The poly(ethylene oxide) head group is non-ionic (N°), and the amine head group (S°) is also uncharged. The non-ionic route ($N^{\circ}I^{\circ}$) seemed to provide greater pore ordering than the neutral route ($S^{\circ}I^{\circ}$), but still lacked long-range hexagonal ordering of the pores. However, this synthesis procedure presents the advantage of using low-cost, nontoxic and biodegradable surfactants.

5.1.4 The Surfactant Packing Parameter

But how is it possible that in some cases honeycomb structures are formed, and in other cases cubic or lamellar structures are formed?

As earlier explained, in a first approximation, it was believed that silica species are simply the negative template of the surfactant. The *soft template*, the micelle, in a hexagonal or cubic form forms the template around which the silica forms. As the template is then burned away, the remaining product is the negative copy of the surfactant. The conditions to form such a cubic phase were very critical, as can be inferred from the phase diagram of CTAB, and this has made it extremely difficult to synthesize MCM-48 in a reproducible way (Figure 5.9).

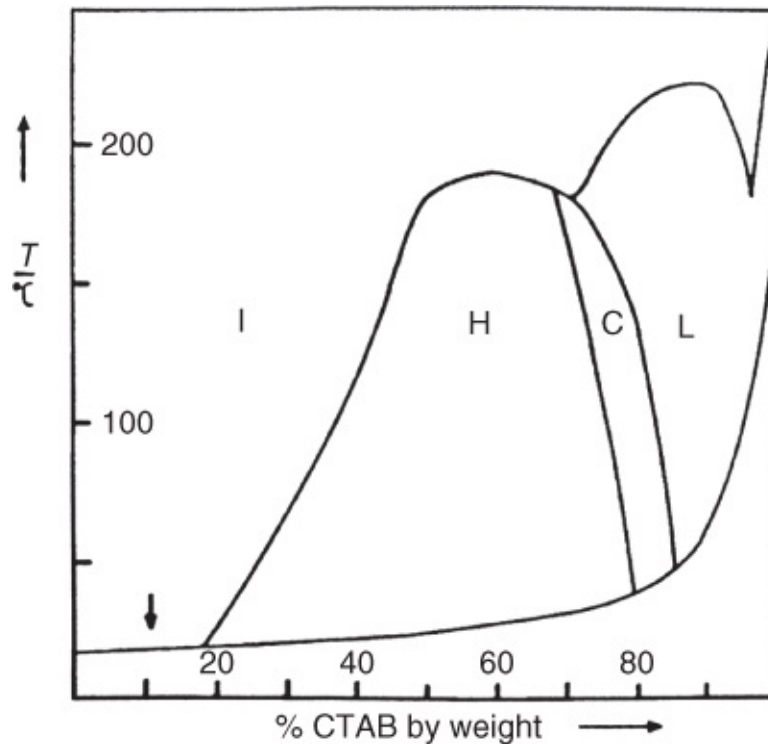


Figure 5.9 Phase diagram of CTAB.

Source: Adapted from Researchgate

([https://www.researchgate.net/post/What is the phase composition of CTAB water and hexanol mixture to get lyo](https://www.researchgate.net/post/What_is_the_phase_composition_of_CTAB_water_and_hexanol_mixture_to_get_lyo))

Several research groups have rationalized the synthesis methods in the past few years and have largely expanded the range of materials that can be prepared. It was soon established that the geometry of the liquid-crystal in pure water does not necessarily reflect the structure of the final inorganic mesophase, and that the mechanism of formation should be regarded as a “cooperative organization” of inorganic and organic molecular species into a three-dimensional array. Jean-Pierre Boilot and coworkers [13] published in 2003 a revised phase diagram that included both the concentration of the surfactant (CTAB) and the concentration of the silica, see [Figure 5.10](#).

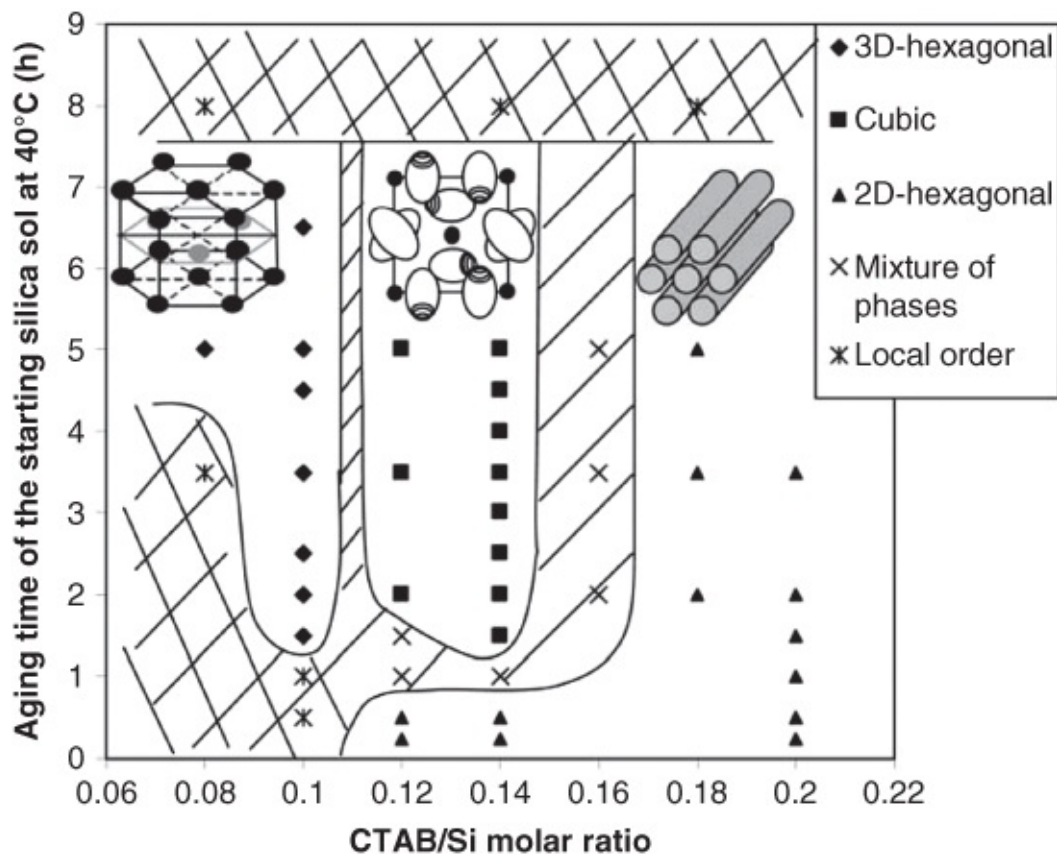


Figure 5.10 Example of a phase diagram for the cooperative mechanism, taking into account both surfactant as silica concentration.

Source: Reproduced with permission of the RSC [13].

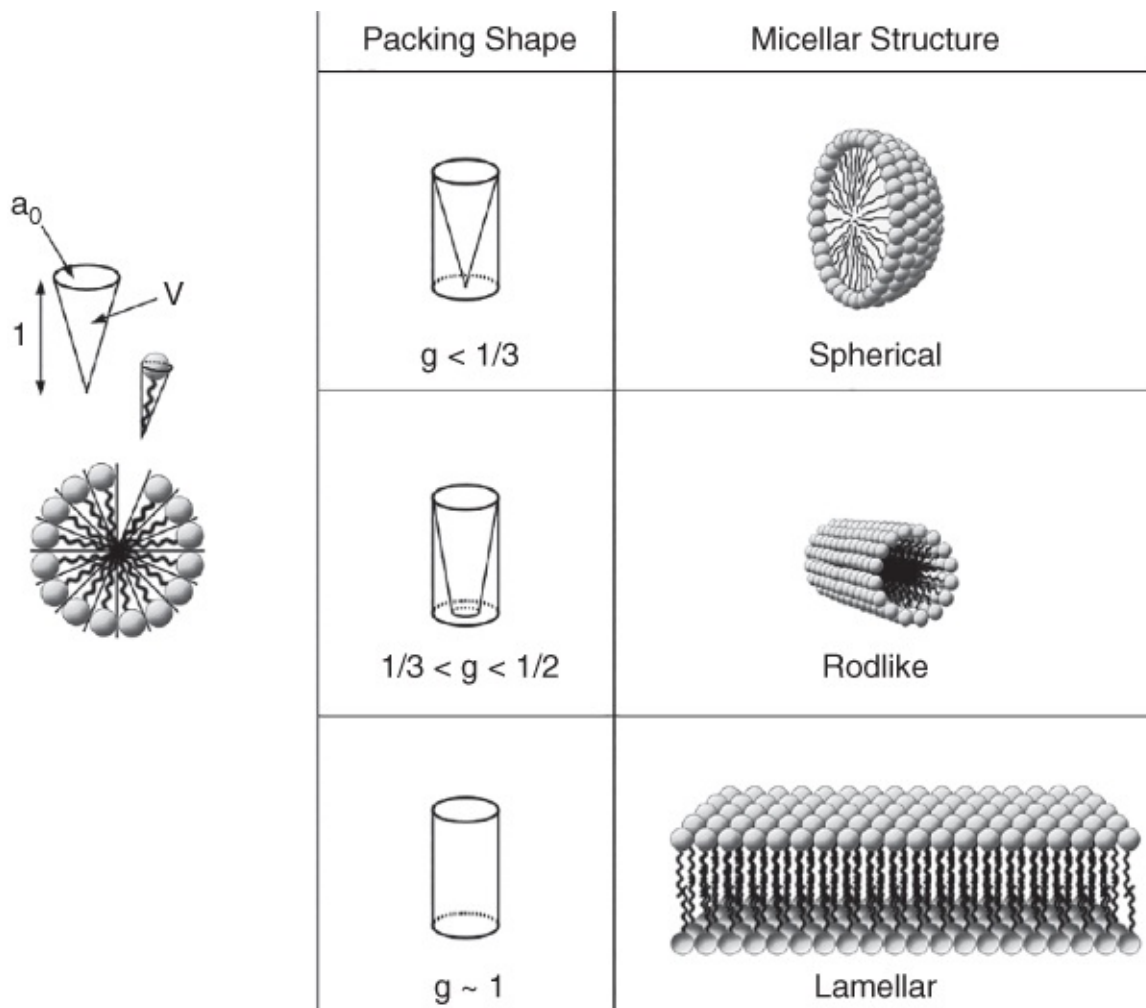
The introduction of the *surfactant ion pair packing parameter*, as a rough “molecular index” to predict the geometry of the mesophase products, can be considered as the first important step in the rationalization of the synthesis routes and the “molecular design” of new mesoporous materials. Whereas, in earlier literature, the ratio surfactant/silica source was claimed to be the major structure-directing parameter, the surfactant packing parameter explains this dependence on a more fundamental level and correlated the shape of the surfactant micelles to the silicate mesophase that is most likely formed.

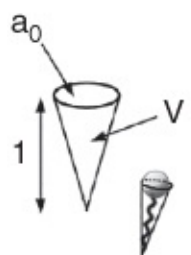




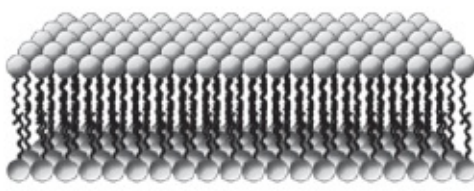
The surfactant packing parameter is defined as

$$g = \frac{V}{a_0 \cdot l} \quad 5.7$$

with V the actual volume of the surfactant, a_0 the area of the headgroup of the micelle, and l the length of the tail (see [Figure 5.11](#)). The surfactant packing parameter is a measure for the shape of the surfactant. Stucky and coworkers [14] discussed in *Science* that, for g -values smaller than one-third, cone-like shapes are created that will pack together to spherical micelles, although a cubic and a 3D hexagonal form can also be formed. Between one-third and half wedge-like shapes are created that will aggregate to the cylindrical hexagonal phase, and surfactants with a g -value above half have a cylindrical shape that will pack together to a

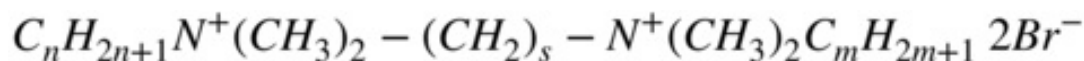
lamellar bilayered structure. In a narrow range between g -values of half and two-thirds, the formation of the cubic phase is possible ([Table 5.1](#)).



Packing Shape	Micellar Structure
 $g < 1/3$	 Spherical
 $1/3 < g < 1/2$	 Rodlike
 $g \sim 1$	 Lamellar

[Figure 5.11](#) The surfactant packing parameter, and its effects of the geometry of the porous material.

An obvious consequence of this was the synthesis of new surfactants that are likely to produce one mesophase in a broad range of synthesis conditions. One example was the development of the so-called *gemini surfactants*, with the general formula



abbreviated to Gem n - s - m . The $(CH_2)_s$ chain is called the *spacer*, which mainly determines the mesophase that is formed; the C_n and C_m *chains* (usually $n = m$) determine the average pore size of the obtained material. In this way, the gemini surfactant GEM-16-12-16 has become very important as an easy and reproducible surfactant to create MCM-48 materials [\[15\]](#).

Table 5.1 The g-value and phase relationship.

g-value	Preferred phase	Example
$<1/3$	Spherical (cubic) (3D-hexagonal)	
$1/3 < g < 1/2$	2D hexagonal	MCM-41, SBA-15
$1/2 < g < 2/3$	Cubic	MCM-48, SBA-16, KIT-6
$2/3 < g < 1$	Lamellar	MCM-50

5.1.5 Hexagonal Mesoporous Silica

In 1995, Peter Tanev and Thomas (Tom) Pinnavaia at Michigan State University published an easier route to obtain hexagonal mesoporous silica (HMS) in *Science* [11]. This route was based on a hydrogen-bonding interaction between a neutral amine and a non-ionic silica precursor. These materials were simply called HMS: Hexagonal Mesoporous Silica. Synthetically, rather than having an anionic-cationic interaction as in the case of the MCM materials (see [Figure 5.8](#), the S^+I^- and $S^+X^-I^+$ interactions), we now have a simple $S^\circ I^\circ$ interaction. A typical synthesis consisted of the use of primary amine, typically $C_{16}-NH_2$, dissolved in a mixture of water and ethanol. The length of the chains determines largely the pore size. To this solution, TEOS is added, and the mixture is stirred and aged at room temperature. After 18 hours, the mixture is poured on a glass plate and air dried. The amine is then removed by washing with hot ethanol. The amine can be recovered and reused.

The HMS materials had a larger stability due to thicker pore walls, as the authors described in their *Science* paper, and a subsequent *Chemistry of Materials* contribution [16]. The HMS materials ($S^\circ I^\circ$) consistently have a large wall thickness than the MCM-41 materials (S^+I^-), whereas the pore size are more or less the same for a similar chain length of the surfactant. In 2000, Cassiers and Van Der Voort [17] reported a method in which the amine template could be simply removed by acidified water. This procedure leads to an immediately usable material, there is no need for a subsequent calcination step. So, a simple synthesis procedure at room temperature, followed by an extraction with acidified water without any other further treatment yield a HMS material with a surface area of $1050 \text{ m}^2 \text{ g}^{-1}$, a pore volume of 0.83 ml g^{-1} , and a pore size of 3.7 nm.



Thomas (Tom) J. Pinnavaia is currently a University Distinguished Professor at Michigan State University. He was an important pioneer in the development of mesoporous silicas, including the MSU-series and HMS. Before that, he was already active in this field, creating mesoporous materials based on Clays. One of these materials were the so-called PCH materials, Porous Clay Heterostructures

(Photo: <http://cit.msu.edu/faculty/pinnavaia.html>).

5.1.6 Stable Ordered Mesoporous Silica – SBA

Although the MCM-41 and MCM-48 were an enormous success, especially in research labs all around the world, the people working on catalysis were still not completely satisfied. The thin and amorphous walls of the MCM-48 and MCM-41 (about 1 nm thick) were relatively unstable. Especially in moist conditions or water, the siloxane bonds are attacked by water (see [Chapter 4](#)) and broken into silanols.

Dongyuan Zhao, currently at Fudan University, but then a post doc with Galen Stucky at Santa Barbara, delivered in 2000 a series of materials that were called the SBA materials (SBA is the acronym for Santa Barbara) [[18](#)]. They had considerably larger pores and considerably thicker walls, the hexagonal variant was called SBA-15 and the cubic variants was called SBA-16. It had a different geometry though to the MCM-48, it was a centrosymmetric cage type structure with the space group $Im\bar{3}m$ (see [Figure 5.12](#)).

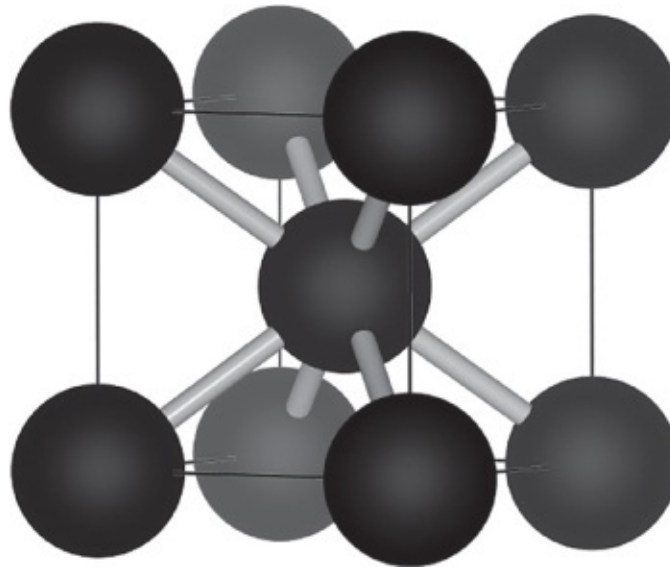
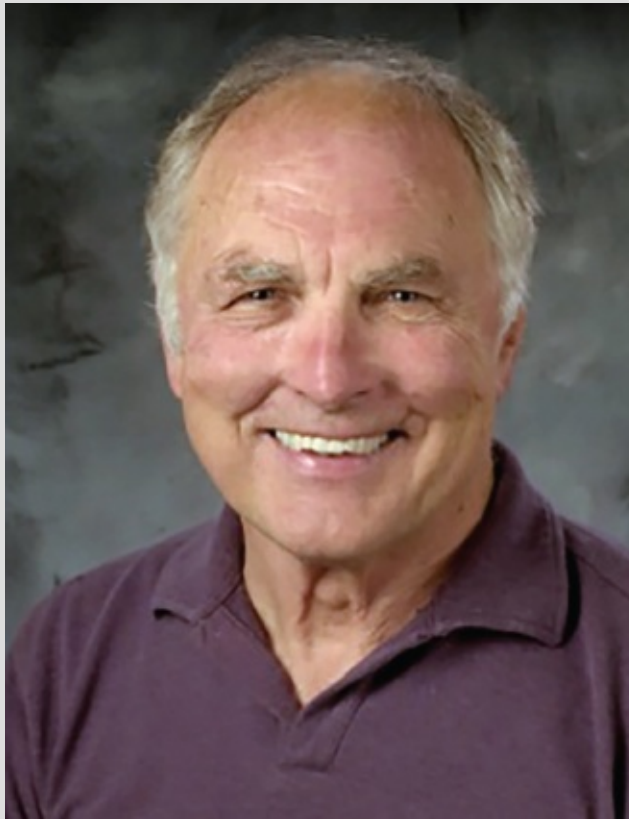


[Figure 5.12](#) Pore structure of SBA-16.



Galen D. Stucky is a Professor at the University of California at Santa Barbara and worldwide respected for his contributions to the field of (meso)porous structured materials. He found many “other” applications for these materials and won in 2008 the ATACCC Award for developing a revolutionary blood-clotting gauze for the military.

Photo: <https://labs.chem.ucsb.edu/stucky/galen/stuckygroup/biography.html>.

The surfactants used were very cheap, non-ionic, and biodegradable “Pluronic[®]” surfactants, a brand name of BASF, for a series of polyethyleneglycol – polypropyleneglycol –

polyethyleneglycol (PEG-PPG-PEG) block-copolymers (Figure 5.13). Just as in the case of the MCM-41 and MCM-48 materials, the *g*-value of the surfactant and the surfactant/silica ratio will determine the final pore geometry.

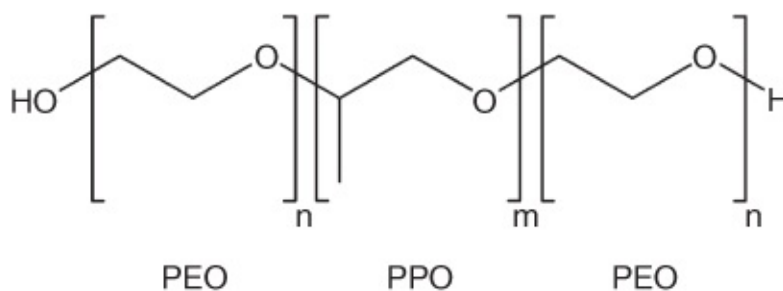


Figure 5.13 Non-ionic triblock copolymer (Pluronic) with large poly(ethylene oxide) (PEO) and poly(propylene oxide) (PPO) blocks.

The Pluronic P123 stands for $(\text{PEG})_{20}-(\text{PPG})_{70}-(\text{PEG})_{20}$ block copolymer. The nomenclature needs some explanation: the “P” stands for “paste,” the aggregation form of the surfactant. (Other letters are “F” for “flakes” and “L” for “liquid.”) If you multiply the first two numbers by a factor of 300, you will get the average molar mass, so in this case P123 has a molar mass of $12 \times 300 = 3600 \text{ g mol}^{-1}$; and the last number, multiplied by 10 gives the weight percentage of the hydrophilic groups (so the PEG groups), this would be in this case 30%.

Another famous one is the F127 that has a formula of $(\text{PEG})_{100}-(\text{PPG})_{65}-(\text{PEG})_{100}$. This much more hydrophilic surfactant is typically used for the creation of the cubic SBA-16. This can be rationalized again by the surfactant packing parameter. The much smaller hydrophobic core compare to the hydrophilic tails yields a packing parameter much smaller than 1 and favorable for cubic structure. Note that the P123 had on the contrary a very large hydrophobic core in comparison to the hydrophilic tails leading to large *g*-values and thus a hexagonal packing. F127 comes in the form of flakes, has an average molar weight of 3600 g mol^{-1} and has a weight percentage of hydrophilic groups of 70%.

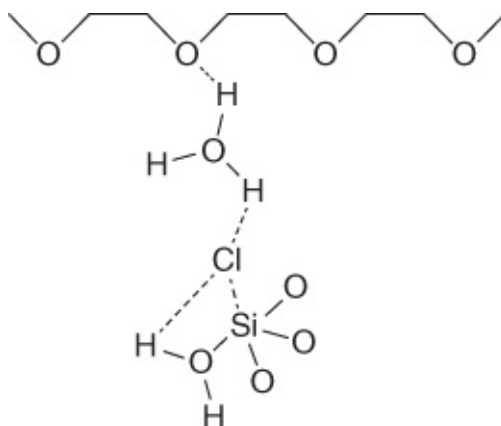
As shown in Table 5.2, the pore size and wall thickness of the SBA-15 is the double of these of the MCM-41, rendering the SBA variants more stable in water and air [19]. They can host much larger molecules, which is very important in the field of adsorption and catalysis.

Table 5.2 Basic physical properties of mesoporous MCM-41 and SBA-15 silicas.

Mesoporous silicas	Surface area ($\text{m}^2 \text{ g}^{-1}$)	d_{100} (nm)	Unit cell (a_0) (nm)	Pore size (nm)	Wall thickness (nm)
MCM-41	1028	3.83	4.42	2.65	1.77
SBA-15	680	8.16	9.42	5.90	3.52

Next to these differences, a very important difference is the fact that for the SBA-type materials, the walls themselves are microporous, because they are perforated. This is due to the specific interaction of the silica precursor with these long tail surfactants.

Let us take the case of SBA-15. The P123 surfactant forms a hydrophobic core of the (PPG)-block, and the more hydrophilic (PEG) blocks stick out and interact with the silica precursors and the formed silicates. In the typical acid conditions of the synthesis (there are also recipes for basic conditions), these hydrophilic PEG blocks interact with the silica according to a $S^0H^+X^-I^+$ interaction as shown in [Figure 5.14](#). The surfactant should be regarded as a hydrophobic core with hydrophilic micelles sticking out and penetrating through the silica that is formed around them. This renders the SBA-type materials highly microporous.



[Figure 5.14](#) Interaction between PEG and silica in acid media.

We show this in [Figure 5.15](#).

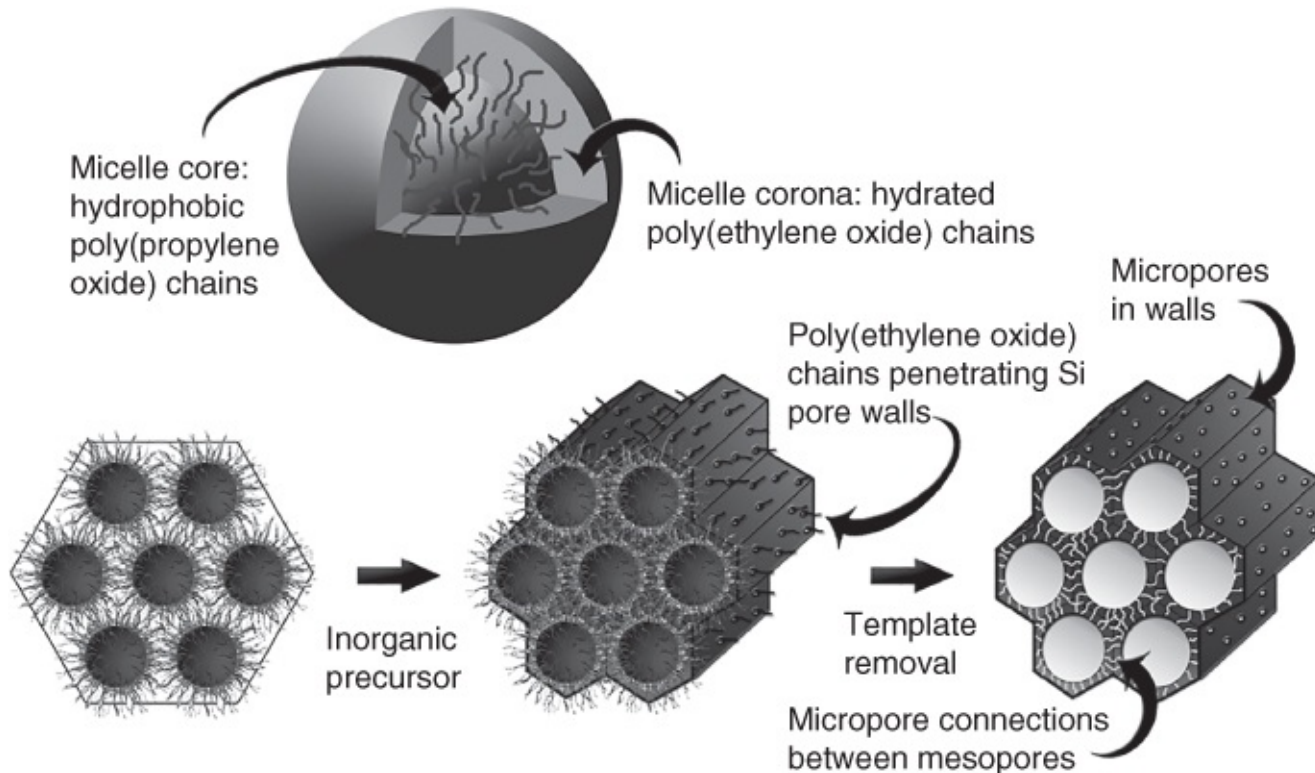


[Figure 5.15](#) Micelle structure of PEO-PPO-PEO triblock copolymers.

Source: Courtesy of Carl Vercaemst.

Anne Galarneau et al. [20] explained in a very visual paper in 2007 how researchers can tune the parameters of the synthesis or post-treatment to tune the pore size of the SBA-15, but also the amount and pore size of the micropores and the wall thickness. The SBA-15 and SBA-16 are therefore not only very stable, but they have a tunable combination of micropores and mesopores and can thus be referred to as *hierarchical porous materials*, a term reserved for materials that have at least two distinct different pore sizes. See [Figure 5.16](#) showing three SBA-15 materials, synthesized at different conditions. The mesopores can then act as the “highways,” guaranteeing fast transport of molecules without any diffusional limitations and the micropores (functionalized or not) can then act as “catalytic pockets” or “adsorption nests.”

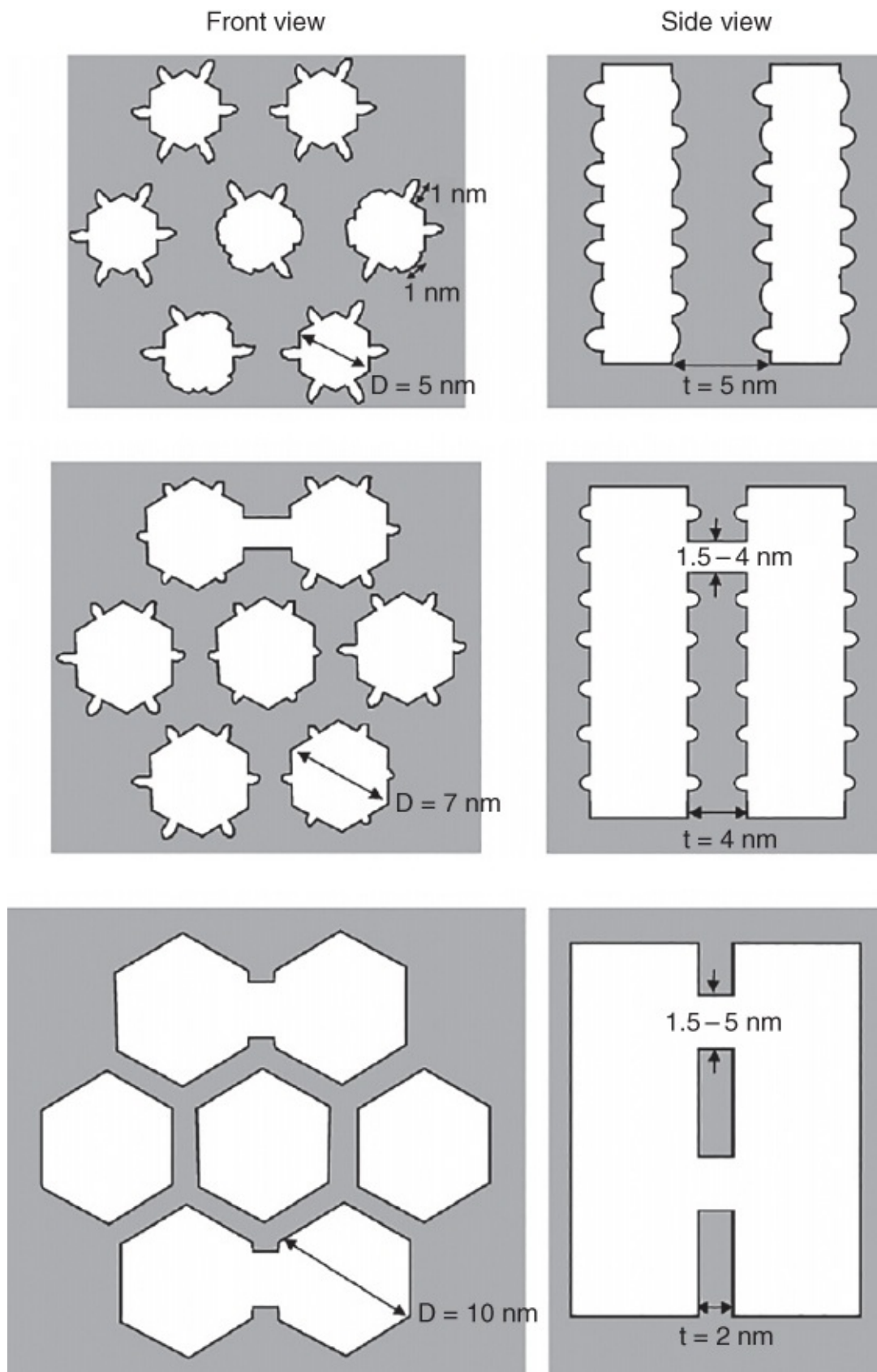
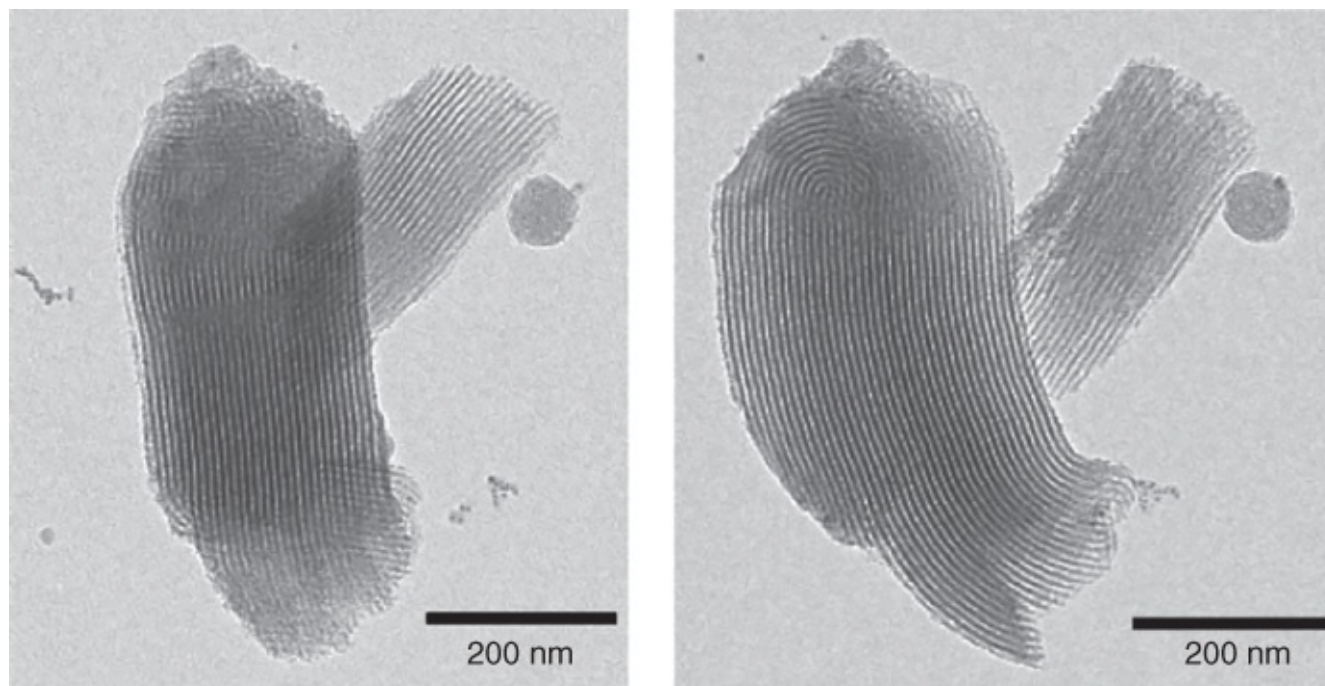


Figure 5.16 Schematic representation of three SBA-15s synthesized in different conditions (Temperature = 60, 100, and 130 °C), revealing different pore diameters, wall thicknesses, microporosities, and interconnections between the main channels.

Source: Reproduced with permission of ACS [20].

On a side note, usually SBA-15 materials are drawn in the literature as short and rigid and straight honeycomb ordered pores. This is not entirely the case. In collaboration with Krijn De Jong at Utrecht University, we published TEM pictures showing the curvatures in real SBA-15 (and other) samples [21]. Some of these TEM pictures are shown in [Figure 5.17](#).



[Figure 5.17](#) TEM pictures of SBA-15, showing the curvature in the pores [21].

Source: Reproduced with permission of the RSC.

Other, but less studied, SBA materials are SBA-11 (cubic, $Pm\bar{3}m$) and SBA-12 (3D-hexagonal, $P6_3/mmc$) [22]. These are usually synthesized using the commercially available surfactants Brij 56 ($C_{16}EO_{10}$) and Brij 76 ($C_{18}EO_{10}$), respectively.

5.1.7 Plugged Hexagonal Templated Silica

In 2002, Van Der Voort et al. [23,24] reported a remarkable isotherm that was never published earlier. The isotherm is shown in [Figure 5.18](#) as type (C).

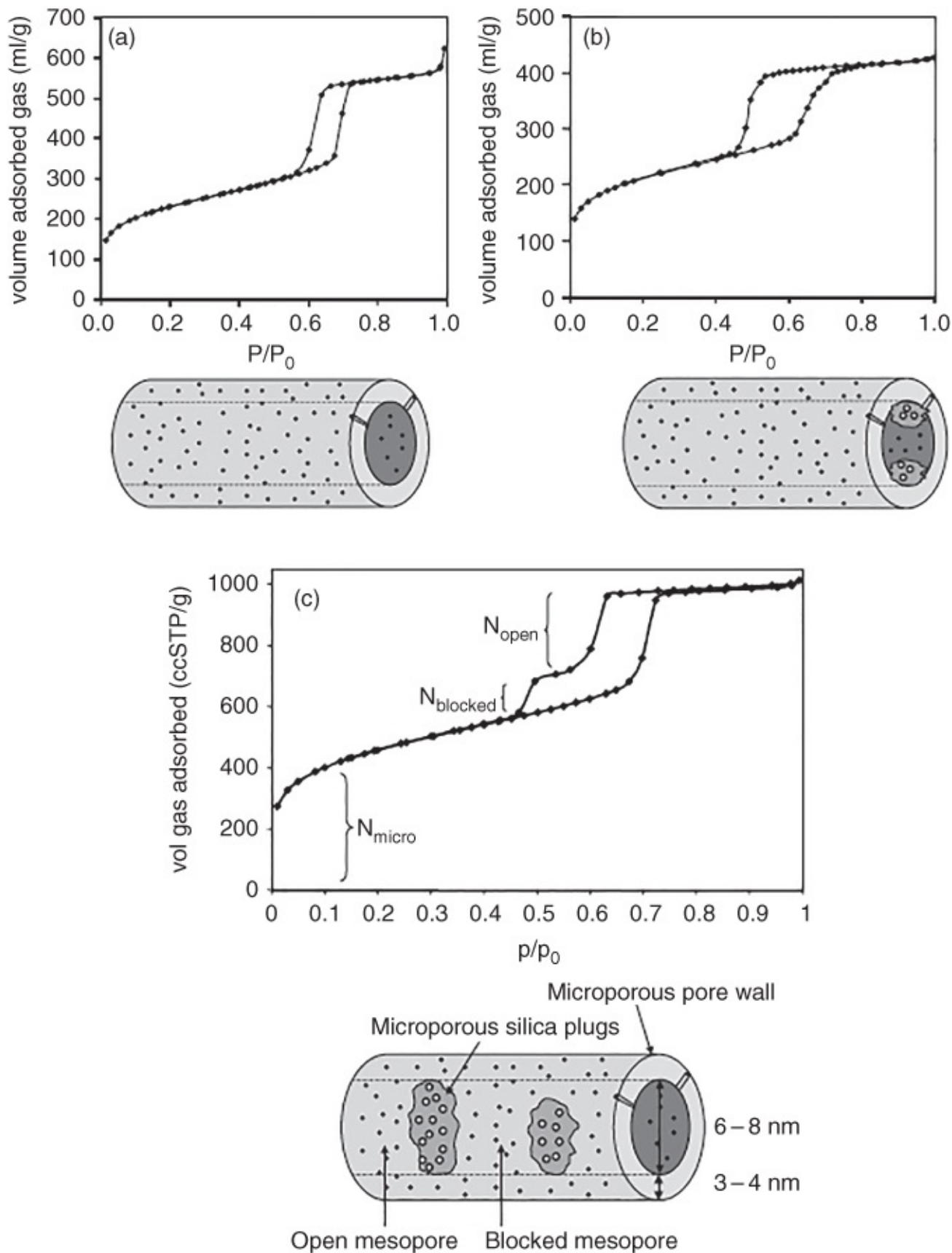


Figure 5.18 Isotherms of (a) open pores; (b) blocked or inkbottle pores and (c) “plugged” pores.

Source: Reproduced with permission of ACS [23].

Type (A) isotherm in [Figure 5.18](#) represents the classic isotherm of the open cylindrical pore case in the SBA-15. According to the IUPAC classification [25], this is an isotherm type IV(a), with a hysteresis loop type H1.

Type (B) isotherm in [Figure 5.18](#) represents the typical case of “cavitation” (see [Chapter 2](#)), the hysteresis loop is forced to close at $P/P_0 = 0.42$, the cavitation pressure of liquid nitrogen at 77 K, below which no stable meniscus of liquid nitrogen is possible. It represents the “inkbottle” pore and is classified by IUPAC as a type IV(a) with a hysteresis loop H2(a).

At the time that Van Der Voort published the isotherm (C), this type of isotherm was not known and not indexed by IUPAC, who used a previous classification of isotherms in the period 1985–2015 [26]. The material was prepared as a regular SBA-15, but with a largely increased silica concentration. The isotherm (C) is remarkable. Combined with the typical $P6mm$ XRD pattern for a hexagonal ordered structure, the following characteristic features can be observed: (i) adsorption in intrawall micropores at low relative pressures; (ii) multilayer adsorption in regular mesopores and capillary condensation in narrow intrawall mesopores; (iii) a one-step capillary condensation, indicating uniform mesopores; (iv) a two-step desorption branch indicating the pore blocking effects (sub-step at the relative pressure of around 0.42). The adsorption–desorption behavior is consistent with a structure comprising both open and blocked cylindrical mesopores. The high-pressure desorption step corresponds to nitrogen desorption from open pores. The blocked pores will remain filled until the vapor pressure is lowered below the “magical” point $p/p_0 = 0.42–0.45$, after which a spinodal decomposition of the condensed nitrogen will occur and these sections will spontaneously empty.

The authors called this material PHTS; Plugged Hexagonal Templated Silica. The capillary condensation process and the cavitation is visualized in [Figure 5.19](#).

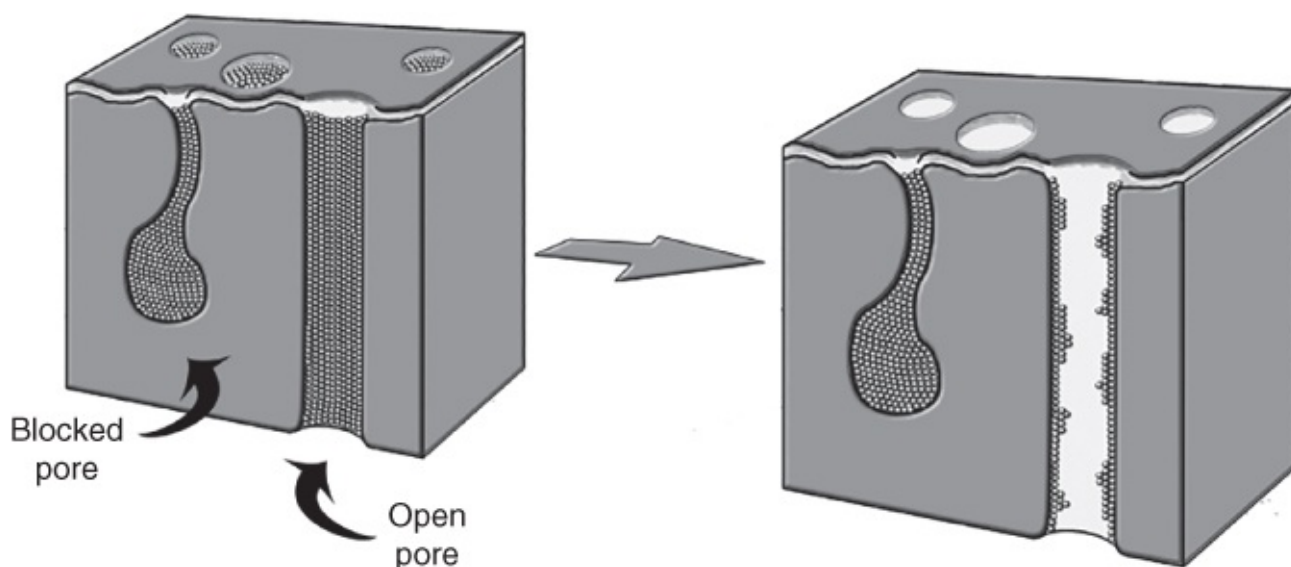


[Figure 5.19](#) Open versus blocked pores in PHTS.

The open versus corrugated and blocked material is also clearly visible from the TEM recordings in [Figure 5.20](#).

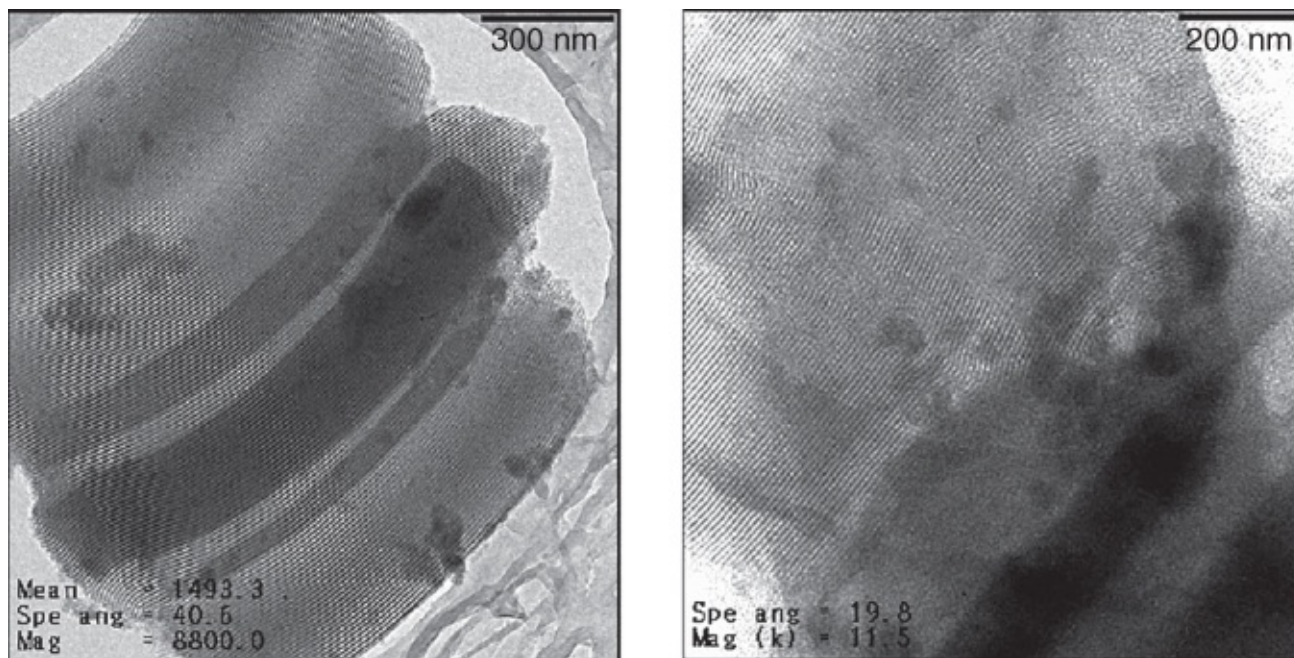


[Figure 5.20](#) TEM images of (left) regular SBA-15 and (right) the PHTS.

Source: Reproduced with permission of ACS [\[23\]](#).

In the same paper, the authors made a comparison of the hydrothermal stability of a wide range of mesoporous silica materials, as visualized in [Figure 5.21](#). The description of the treatments is as follows: “Mild” samples are treated in a nitrogen flow (25% water) at 1013 hPa and 673 K for 50 hours; “Medium” samples are treated in a nitrogen flow (25% water) at 1013 hPa and 673 K for 120 hours; “Hard” samples are steamed on a grid above the water in an autoclave at 393 K and autogenous pressure for 24 hours.

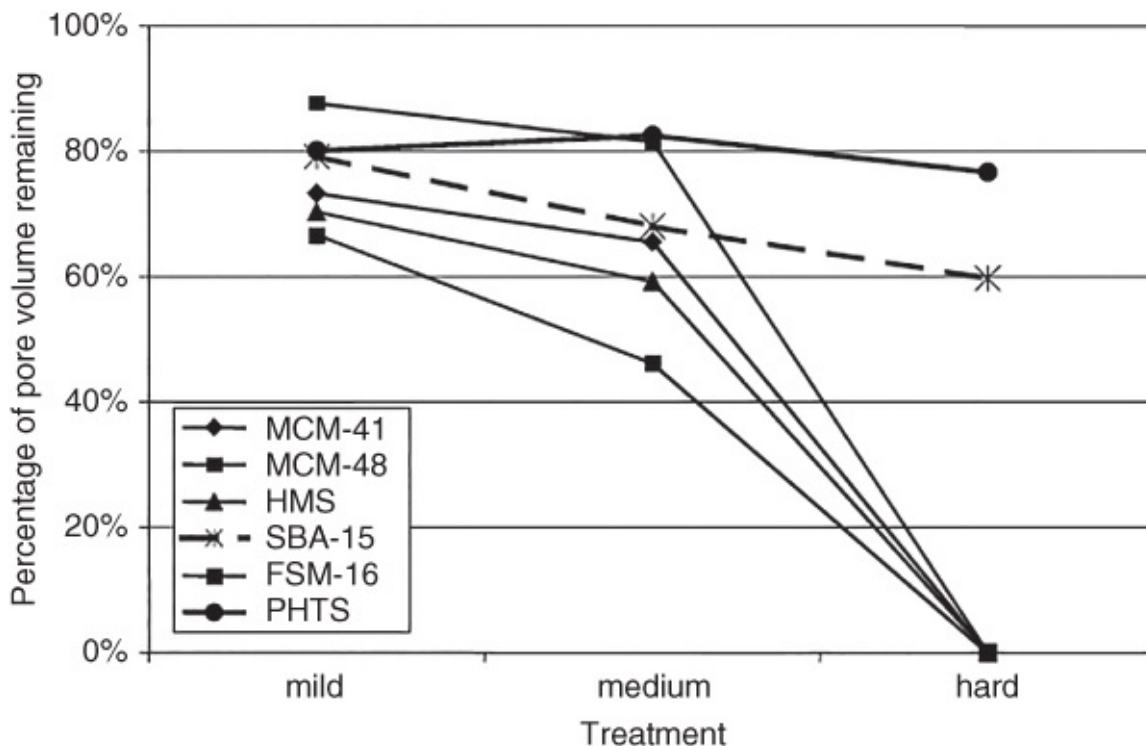


Figure 5.21 Comparison of the hydrothermal stability of several mesoporous silicas. The terms hard, medium, and soft are defined in the text.

Source: Reproduced with permission of ACS [23].

It is remarkable that only the SBA-15 and the PHTS materials survive this harsh treatment. All other materials collapse.

In 2015, IUPAC classified this new hysteresis profile as hysteresis loop H5 [25].

5.1.8 The New MCM-48: KIT-6

As argued before, the synthesis of MCM-48 is not too easy, it requires either a very narrow set of conditions using the regular ammonium-based surfactants, or the use of non-commercially available gemini surfactants.

Much later, in 2003, Freddy Kleitz, Ryong Ryoo, and coworkers [27] (Korea Advanced Institute of Science and Technology) published a novel pathway to make the $Ia\bar{3}d$ cubic mesoporous silica more easily, in *Chemical Communications*; they called it KIT-6 (KIT standing for the Korea Institute of Technology). They created a large pore high quality $Ia\bar{3}m$ cubic material by the simple addition of butanol to an acidified solution of P123. Remember that the molecular structure of P123 typically yielded hexagonal SBA-15 because of its high g -value. The authors reasoned that the addition of butanol is responsible for the preferred swelling of the hydrophobic volume of the block-copolymer micelles, leading first to the formation of micellar aggregates with a decreased curvature (lamellar mesophase). The lamellar form was made previously (so-called MCM-50), but has not been followed up much in the literature, as these structures have no applications; the lamellar phase is formed for g -values in between the hexagonal and the cubic phase.

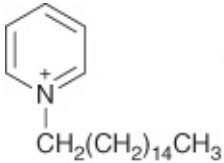
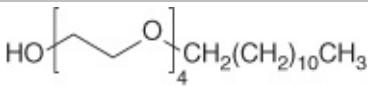
Upon further reaction or increased temperature, the further condensation of the silicate region provokes folding and regular modulation of the silica surface, inducing significant changes in the micelle curvature. The interplay of the silicate formation and the micelle curvature was known previously (the cooperative mechanism), but this was the first time it was observed for a non-ionic surfactant.

5.1.9 Further Developments of Mesoporous Silica

Since the publication of the M41S type materials, thousands of papers have appeared on alternative preparations of porous silicas, using different surfactants, different ingredients, other structures, and so on.

It is impossible to cover all these papers, even in such a comprehensive book as this one. We can give an overview of the most important applications though. [Table 5.3](#) shows an overview of the surfactants that have been often used in the synthesis of mesoporous silicas. The CTAB was the original surfactant for the synthesis of MCM-41, but several other cationic surfactants have been used as well. Among the non-ionic surfactants, we have already discussed the amphiphilic triblock copolymers such as P123 and F127. Another popular class of surfactants for mesoporous silica synthesis are the Brij[®] surfactants. Brij surfactants are also amphiphilic, and non-ionic, they are polyethylene glycol alkyl/aryl ethers. They act very similar to the triblock copolymers.

[Table 5.3](#) List of frequently used surfactants in PMO synthesis.

Abbreviation	Full name	Structural formula
CTAC/CTAB	Cetyltrimethylammonium chloride/bromide	$\begin{array}{c} \text{CH}_3 \\ \\ \text{H}_3\text{C}-\text{N}^+-\text{(CH}_2\text{)}_{15}\text{CH}_3 \\ \\ \text{CH}_3 \end{array} \quad \text{Cl}^-/\text{Br}^-$
OTAC	Octadecyltrimethylammonium chloride	$\begin{array}{c} \text{CH}_3 \\ \\ \text{H}_3\text{C}-\text{N}^+-\text{(CH}_2\text{)}_{17}\text{CH}_3 \\ \\ \text{CH}_3 \end{array} \quad \text{Cl}^-$
C _n TMACl/Br	Alkyltrimethylammonium chloride/bromide	$\begin{array}{c} \text{CH}_3 \\ \\ \text{H}_3\text{C}-\text{N}^+-\text{(CH}_2\text{)}_{n-1}\text{CH}_3 \\ \\ \text{CH}_3 \end{array} \quad \text{Cl}^-/\text{Br}^- \quad (n = 8, 10, 12, 14, 16, 18)$
CPCI	Cetylpyridinium chloride	
FC4	Fluorocarbon surfactant	$\text{C}_3\text{F}_7\text{O}(\text{CFCF}_2\text{CF}_2\text{O})_2\text{CFCF}_2\text{CONH}(\text{CH}_2)_3-\text{N}^+(\text{C}_2\text{H}_5)_2 \quad \text{Cl}^-$
Brij-30	Polyoxyethylene (4) lauryl ether	

Brij-56	Polyoxyethylene (10) cetyl ether	
Brij-76	Polyoxyethylene (10) stearyl ether	
Triton-X100	Polyoxyethylene (10) octylphenyl ether	
P123	Pluronic P123 Poly(ethylene glycol)-poly(propylene glycol)-poly(ethylene glycol)	
F127	Pluronic F127 Poly(ethylene glycol)-poly(propylene glycol)-poly(ethylene glycol)	
B50-6600	Poly(ethylene oxide)-poly(butylene oxide)-poly(ethylene oxide)	
PEO-PLGA-PEO	Poly(ethylene oxide)-poly(lactic acid-co-glycolic acid)-poly(ethylene oxide)	
C _{n-s-m}	Divalent and gemini surfactants	

When using non-ionic structure direction agents (SDAs) such as triblock copolymers, inorganic salts will exhibit a special effect during the Periodic Mesoporous Organosilica (PMO) assembly by influencing the interaction between several parts of the polymer [28]. The salt causes a dehydration of the hydrated ethylene oxide units of the polyethylene oxide (PEO) chain, which is located next to the polypropylene oxide (PPO) chain. This results in an increased hydrophobicity of the PPO chain and significantly decreases the hydrophilicity of PEO. Many salts have shown to improve the hydrothermal stability of during the crystallization process (e.g. NaF, NaCl, KF, KCl, Na₂SO₄, ...) [18,29]. It also allows us to prepare highly ordered materials in a wide range of acidic concentrations.

The addition of KCl significantly increases the interaction between the SDA and the polysilsesquioxane and weakens the disordering of the organic units. It especially improves the interaction between the non-ionic block copolymer and the oligomers of the precursor

that are formed during hydrolysis and condensation.

5.1.10 Pore Size Engineering

An important aspect of tailoring a mesoporous silica is the ability to enlarge the pore size. This is called *pore size engineering*. Particularly for applications such as the immobilization or adsorption of proteins, enzymes or drugs, this is of major importance. The employment of block-copolymers and poly(alkylene oxides) already resulted in larger pores, however values above 10 nm could not be achieved. As we discussed earlier, tuning the synthesis conditions is an important tool to engineer the pore sizes. But still the limit seems to be about 10 nm.

The addition of swelling agents to the reaction mixture is the solution for this issue. These additives are typically hydrophobic compounds that will interact with the surfactant by settling in the hydrophobic part of the polymer. An expansion of the hydrophobic core of the surfactant will occur and this results in larger pores. Typical swelling agents are 1,3,5-trimethylbenzene (TMB), 1,3,5-triisopropylbenzene (TPB), cyclohexane, dodecane, and poly(propylene glycol), but xylene, toluene, and benzene have also been reported. With the aid of TMB, the pore sizes can be enlarged to about 40 nm in acidic triblock copolymer systems (say the SBA-type materials) and to 10 nm in basic CTAB (MCM-type materials) conditions. There is a price to pay: the materials lose order and become more disordered, although the pore size remains uniform.

[Table 5.4](#) gives an overview of the strategies to obtain a certain pore size [30].

[Table 5.4](#) Strategies to obtain materials with a certain pore size.

Pore size (nm)	Method
2–5	Surfactants with different chain lengths including long-chain quaternary cationic salts and neutral organoamines
4–7	Long-chain quaternary cationic salts as surfactants High-temperature hydrothermal treatment
5–8	Charged surfactants with the addition of organic swelling agents such as TMB and midchain amines
2–8	Non-ionic surfactants
4–20	Tiblock-copolymer surfactants
4–11	Secondary synthesis, for example water-amine postsynthesis
10–30	High molecular weight block-copolymers, such as PI- <i>b</i> -PEO, PIB- <i>b</i> -PEO, and PS- <i>b</i> -PEO Triblock copolymers with the addition of swelling agents TMB and inorganic salts Low-temperature synthesis

5.1.11 Making Thin Films – The EISA Principle

The true liquid-crystal templating and the cooperative self-assembly are not suitable for the deposition of highly uniform thin films. Therefore, the evaporation-induced self-assembly (EISA) has been developed by Brinker's group [31] (Figure 5.22). In the EISA approach, an excess of a volatile solvent is used to ensure that the surfactant concentration in the solution remains below the CMC. Additionally, the solution must be consisted of solvents and reactants which are highly volatile. Since less condensed entities (small and mobile) are preferred during self-assembly, it is important to choose conditions that favor hydrolysis but hinder condensation of the inorganic species.

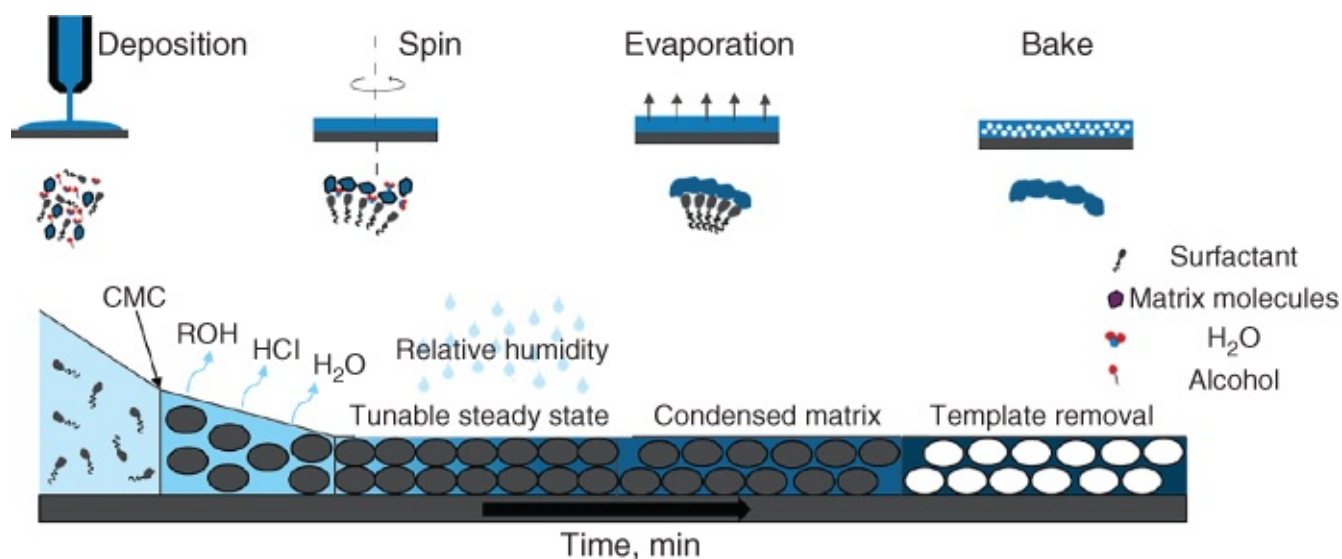


Figure 5.22 Formation of mesoporous films via the EISA.

Through variation of the initial alcohol/water/surfactant/matrix precursor mole ratio it is possible to follow different trajectories in composition space and to arrive at different final mesostructures [31a]. Upon addition of the solution to the substrate, the preferential evaporation of the volatile solvent during dip- or spin-coating concentrates the depositing film in nonvolatile surfactant and silica species. The evaporation of the volatile species is one of the main parameters that governs the entire film-formation process. When the surfactant concentration reaches the equivalent of the CMC for the system, micelles start to form. Eventually, an organized mesostructure film is obtained. The main challenge of the EISA compared to the previously described precipitation methods is that it is a mainly kinetically governed mechanism that requires high control of the processing conditions, and it can lead to metastable hybrid materials that require additional steps for stabilization. The quality of the final mesostructure is thus highly dependent on the processing conditions and more especially on the atmosphere composition (water and solvent relative pressures), since the latter defines the evaporation rate and the system content in water and solvent at equilibrium.

5.2 Applications of Mesoporous Silica

5.2.1 In Heterogeneous Catalysis – Functionalization of Mesoporous Silica

One of the most explored applications of the mesoporous silicas is the field of heterogeneous catalysis. It was one of the primary reasons to develop these types of materials in the early 1990s. Therefore, the first efforts in the field of heterogeneous catalysis wanted to exploit the larger pore sizes of the catalysts to convert larger substrates that could not enter the pores of zeolites and zeotypes. As the pores of the ordered mesoporous silicas are relatively uniform, researchers also investigated the *shape selectivity* in the catalytic process.

5.2.1.1 Functionalization of the Mesoporous Silica

A plethora of methods for preparing catalysts is available.

5.2.1.1.1 Metal Doping

Very similar to zeolite synthesis, mesoporous silicas can be doped with hetero-elements. The most often used dopants are Al^{3+} and Ti^{4+} , but many other dopants have been used in the past decades. The most used method is to add a hydrolysable metal salt to the synthesis mixture; alkoxides or chloride salts are often used. One has to choose the metal compound in such a way that the hydrolysis rate of the metal compound is in the same range as the silicon source. A rule of thumb is that the larger the alkoxy group is, the slower the hydrolysis occurs. For example, as Ti-alkoxides are much more reactive than the silica counterparts, a typical match is found by mixing TEOS (ethoxy ligands) with $\text{Ti}(i\text{OPr})_4$ (isopropoxy ligands, to slow down the hydrolysis rate).

Al-ions are typically introduced using $\text{Al}(i\text{OPr})_3$, aluminum chloride, hydroxide, or the sulfate. The introduction of aluminum created both Lewis and Brønsted acid sites in the material.

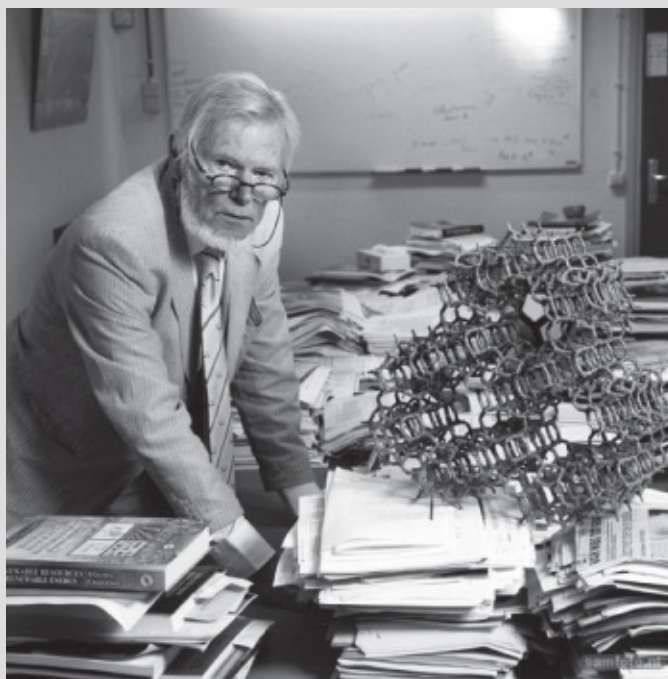
As an early example, Avelino Corma et al. [32] systematically investigated the catalytic cracking performance of gas oil of an Al-MCM-41 with varying Si/Al ratios (Si/Al = 14, 100, 143). Just as in zeolites, acid catalysts are created this way. The authors compared these catalysts with the more classical ones, being Ultra Stable Y (USY)-zeolite (Si/Al = 100) and amorphous silica-alumina (Si/Al = 2.5). Two main conclusions were drawn from this work: (i) the less Al^{3+} is added, the stronger these sites are (also observed in zeolites) and (ii) while the USY is 139 times more active than the Al-MCM-41 for small molecules (*n*-heptane), the USY was 11 times less active than the Al-MCM-41 for large molecules (gas oil). These values confirmed the size-exclusion effect in zeolites: the large gas oil molecules cannot penetrate the pore system of the USY. Still the catalytic activity of the semi-amorphous Al-MCM-41 is much lower in an equal-level playing field.



Avelino Corma is a Spanish chemist, who is internationally recognized for his leading research on heterogeneous catalysis. He is Professor at the Institute of Chemical Technology (ITQ-CSIC-Polytechnical University of Valencia). He has published more than 900 research papers and is inventor on more than 100 patents. Over 12 of those patents have been applied industrially in commercial processes of cracking, desulfuration, isomerization, epoxidation, chemo selective oxidation of alcohols, and chemoselective hydrogenations.

Photo: <https://commons.wikimedia.org/wiki/File:Avelino-Corma.jpg> (public domain).

It is also possible to create basic catalysts, typically by ion-exchange – that is, exchanging the acid mobile protons, just as in zeolites – with Na or Cs ions. Van Bekkum and Kloetstra [33] made such catalysts and prepared Na-MCM-41 and Cs-MCM-41. In particular, the Cs-exchanged catalyst showed some superbase properties and was not only active in the typical Knoevenagel condensation, but also in the more demanding Michael addition.



Herman van Bekkum is a Dutch (organic) Chemist who became one of the pioneers of heterogeneous catalysis in zeolites and later also on heterogeneous catalysis using mesoporous materials. He has been the Rector Magnificus at the Technical University of Delft and has been a researcher at the Royal Dutch Shell Oil Company. He has been knighted in the Netherlands for his contributions.

Photo: <http://www.delta.tudelft.nl/article/herman-van-bekkum>.

Doping with transition metals then typically yields oxidation catalysts. The benchmark in oxidation catalysis on industrial scale is the TS-1 (titania silicate) zeolite. It also suffers from small pores. Pinnavaia was one of the first to demonstrate the use of Ti-HMS and Ti-MCM-41 [34]. Just like Corma for the acid catalysis, he corroborated that the TS-1 is the catalyst of choice for small molecules and becomes inactive for molecules exceeding its pore size, and that the Ti-HMS and Ti-MCM-41 are still active for larger molecules.

5.2.1.1.2 One-Pot Synthesis – Co-Condensation

The co-condensation method is a one-pot synthesis procedure. Here, the functionalized silica is prepared through co-condensation of TEOS with functional silanes in the presence structure-directing agent. This is visualized in [Figure 5.23](#). The involvement of the organosilane in the mesostructured formation implies that the chemistry of the functional group has to be taken into account. If not, the organosilane can interfere in the formation of micellar aggregates, leading to disordered amorphous materials. For instance, if the organosilane consists of an amine group, working under acidic conditions implies protonation of this functional group that may interact with silanol groups and prevent direct interaction of the surfactant with the condensating silicate species.

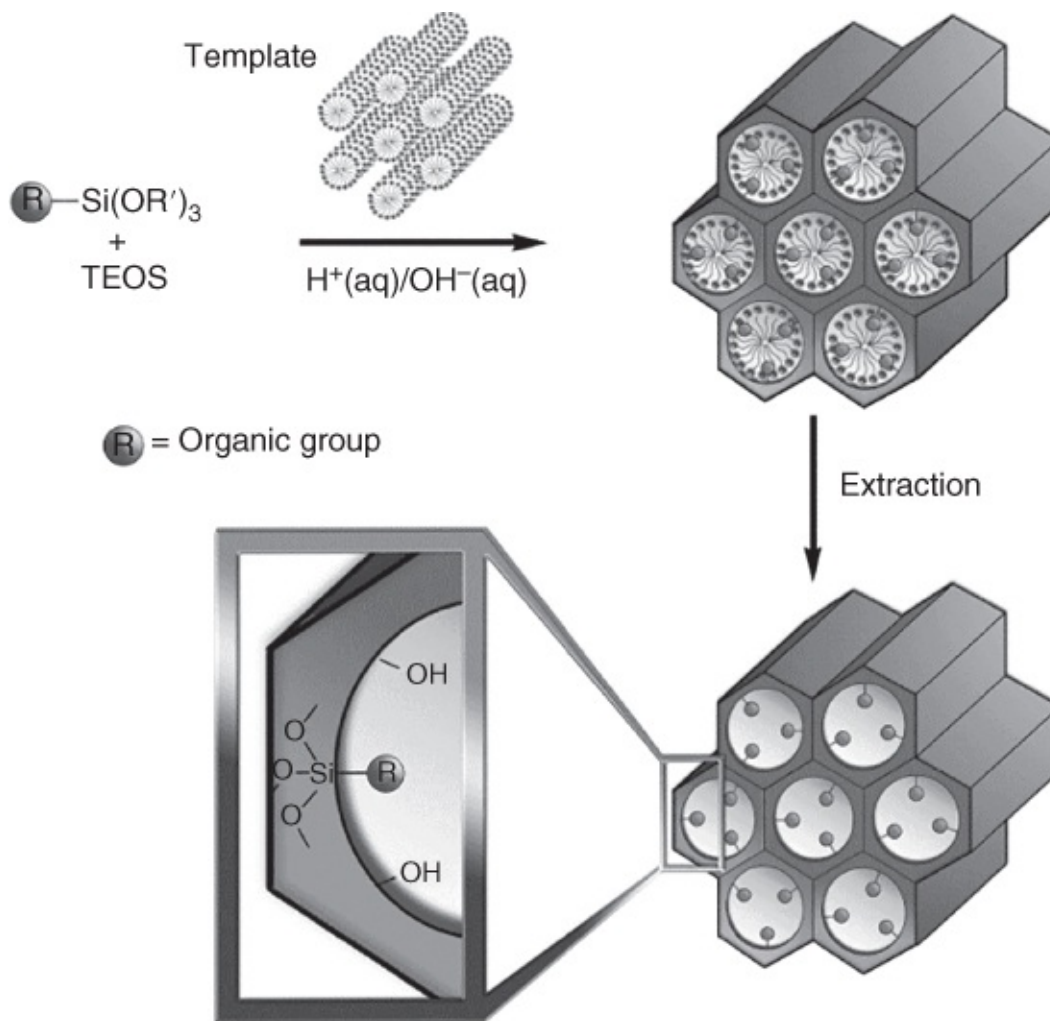


Figure 5.23 Synthesis of functionalized ordered mesoporous silica by means of the co-condensation method.

Source: Figure is redrawn from Fröba's excellent review [35], Reproduced with permission of John Wiley & Sons, Ltd.

As the organic functionalities of these materials are incorporated into the framework during the formation of the mesostructure, they are usually nicely homogeneously distributed throughout the network. However, the homogeneous distribution of the organic units is strongly dependent on the hydrolysis and condensation rates of the silica and organosilica precursors. Rate differences for the hydrolysis and/or condensation of mixed precursors can lead to self-condensation and phase separation.

The co-condensed materials can be used as such, for example, an amine group in a base-catalyzed reaction (Knoevenagel, Henry, aldol-condensation, Michael addition), can be further processed (e.g. the oxidation of a thiol group by a mild oxidant to a sulfonic acid group for acid catalysis), or can be the anchoring point to attach organocatalysts or nanoparticles (NPs) (e.g. gold nanoparticles that attach on thiol functionalities). We refer to an older, but excellent review by M. Davis for a plethora of examples [36].

The main disadvantage of this method, however, is the effect of organic content on the degree of mesoscopic order of the obtained hybrid materials. As the concentration of organosilane increases, the structural ordering of the material decreases and will ultimately lead to a

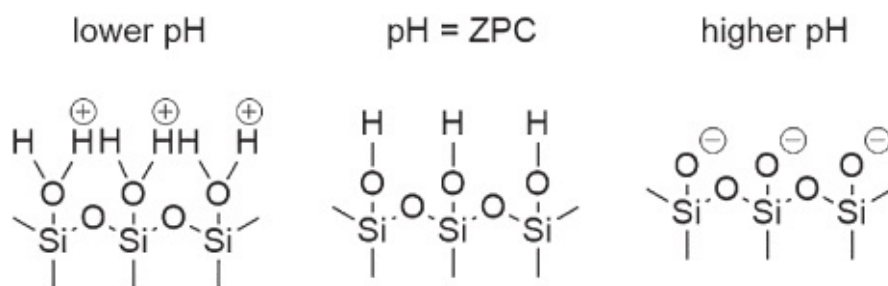
completely disordered solid.

5.2.1.1.3 Dry and Wet Impregnation

Dry impregnation or “pore volume impregnation” or “incipient wetness impregnation” is the impregnation method in which the amount of liquid (solution of the precursors) used is just enough to fill the pore volume of the support. In *wet impregnation* the support is dipped into an excess quantity of solution containing the precursor(s) of the active phase. In practice, these operations are carried out in various ways. In dry impregnation the solubility of the catalyst precursors (usually soluble salts) and the pore volume of the support determine the maximum loading available each time of impregnation. If a high loading is needed, successive impregnations (and heat treatments) may be necessary. When several precursors are present in the impregnating solution simultaneously, the impregnation is called “co-impregnation.”

In the first step of impregnation three processes occur: (i) transport of solute into the pore system; (ii) diffusion of solute within the pore system and (iii) uptake of solute by the pore wall. In the case of wet impregnation, a fourth process is operative, namely transport of solute to the outer particle surface. Dependent on the process conditions, different profiles of the active phase over the particle are obtained. For instance, dependent on the pH, the interaction with the support can be strong or weak, and even repulsion can exist.

Let us consider the not-unusual situation where the solute or its ions are fixed to the support either by reaction or exchange with the surface OH groups and/or by adsorption. In the former case, the concentration (density) of surface OH groups, which depends on the pretreatment of the support, is crucial. In the latter case, the surface charge plays an important role. At a pH value of the so-called *Point of Zero Charge* (PZC) the surface is electrically neutral. At pH values above PZC, the surface is negatively charged, while at pH values below PZC the surface is positively charged ([Scheme 5.23](#)).



[Scheme 5.1](#) Surface of silica at basic, neutral, and acidic pH.

For silica this can be illustrated as follows. At pH = 3 the surface is neutral. In a mildly basic environment, H⁺ ions are removed, and, as a result, the surface is negatively charged. In an acid environment, the surface will become protonated. If you want to deposit anions onto the carrier surface, the preparation should proceed at pH values below the PZC, and for cations you would prefer a pH value above that of the PZC. Alumina has a PZC of around 8. We should mention that the exact PZC values not only depend on the chemical nature of the carrier, but also on its history and the method by which it was prepared. Of course, for the

solid support a window of stability exists.

Impregnation Profiles

For impregnated catalysts a completely uniform profile of the active material over the particle is not always the optimal profile. It is possible to generate profiles on purpose, and in this way to improve the catalyst performance. [Figure 5.24](#) shows four major types of active-phase distribution in catalyst spheres. The gray regions represent the areas impregnated with the active phase. Type (a) is a uniform catalyst while the others have a non-uniform active-phase distribution. They are called “eggshell,” “egg-white,” and “egg-yolk” catalysts. The optimal profile is determined by the reaction kinetics and the mode of catalyst poisoning. For example, an eggshell catalyst is favorable in the case of a reaction with a positive reaction order, whereas an egg-yolk catalyst is the best choice for reactions with negative orders. When pore mouth poisoning is dominant it might be attractive to locate the active sites in the interior of the catalyst particles. Another factor is attrition. If attrition is important and if the active phase is expensive (e.g. precious metals), it might be preferable to place the active phase in the interior of the catalyst particles.

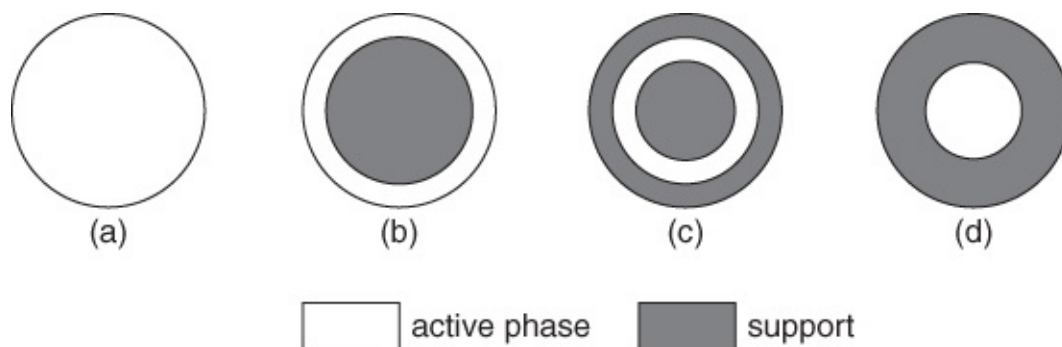


[Figure 5.24](#) Four types of active-phase distribution. (a) uniform, (b) eggshell, (c) egg-white, and (d) egg-yolk.

The addition of a second component to the impregnating solution allows fine-tuning of the catalyst. [Figure 5.25](#) illustrates this. Impregnation of H_2PtCl_6 is carried out in the presence of citric acid, which adsorbs more strongly than H_2PtCl_6 (and HCl). Without the presence of citric acid an eggshell type of profile for Pt is obtained. When some citric acid is present, this will adsorb first and block the outer sphere of the catalyst for the Pt-species. The Pt-species will pass the citric acid outside part and settle in the middle, creating an egg-yolk catalyst.

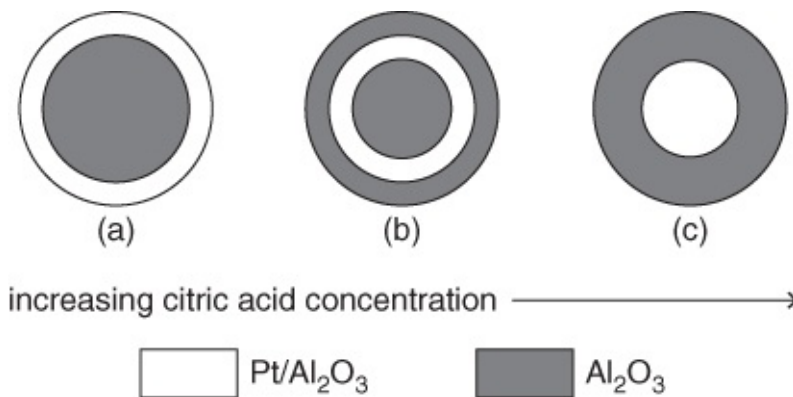


Figure 5.25 The influence of coadsorbing ions (citrate) on the Pt concentration profile.

5.2.1.1.4 Grafting

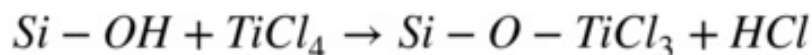
According to the recommendations of IUPAC, “deposition involving the formation of a strong (e.g. covalent) bond between the support and the active element is usually described as grafting or anchoring.”

“This is achieved through a chemical reaction between the functional groups on the support and an appropriately selected inorganic or organometallic compound of the active element.” Other terms like “immobilized,” “heterogenized,” “attached,” and so on are found in literature.

Three classes of coordination metals are used very frequently for direct grafting/anchoring:

- (1) metal halides and oxyhalides (e.g. TiCl_4 , MoCl_5 , CrO_2Cl_2)
- (2) metal alkoxides ($\text{VO}(\text{iPr})_3$) en diketonate complexes ($\text{Cu}(\text{acac})_2$, $\text{VO}(\text{acac})_2$)
- (3) organometallics, especially metal allyls and metal carbonyls ($\text{Cr}(\eta^3\text{-C}_3\text{H}_5)_4$; $\text{Ru}_3(\text{CO})_{12}$).

These types of organometallic complexes typically react with the silica surface, according to



Of course, several side reactions are possible (e.g. reaction with two silanols by the same complex) and the presence of water is detrimental to the reaction, as it will react directly with the very reactive metal complexes.

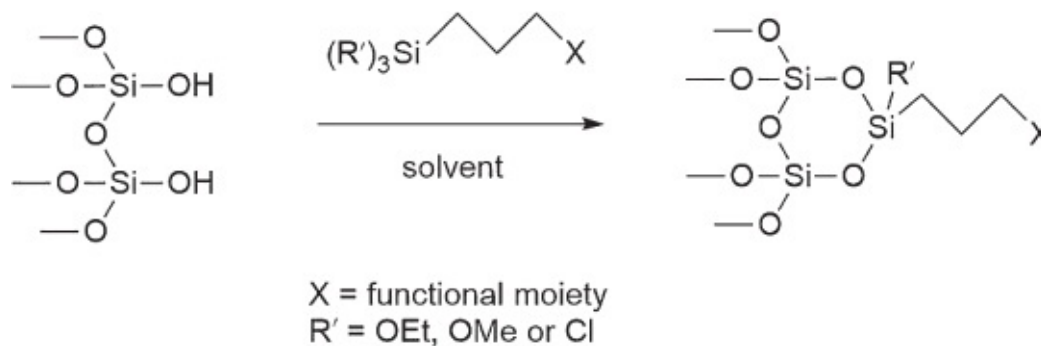
One of the most important problems is the poor stability of most grafted metal complexes on the silica surface in water or polar media. Also, at higher temperatures, the grafted complexes show a high mobility and tend to cluster (coalescence). This is sometimes solved by silylating the surface first.

Silylation of the Silica Surface

Silane coupling agents have the ability to form a durable bond between organic and inorganic

materials. The general formula for a silane coupling agent typically shows the two classes of functionality. X is a hydrolysable group typically alkoxy, acyloxy, halogen, or amine. Following hydrolysis, a reactive silanol group is formed, which can condense with other silanol groups – for example, those on the surface of silica – to form siloxane linkages.

The R group is a non-hydrolysable organic function. The result of reacting an organosilane with a substrate is shown in [Scheme 5.25](#).



[Scheme 5.2](#) Example of grafting organosilanes onto a silanol-containing surface.

Most of the widely used organosilanes have one organic substituent and three hydrolysable substituents. In the majority of surface treatment applications, the alkoxy groups of the trialkoxysilanes are hydrolyzed to form silanol-containing species. Reaction of these silanes involves four steps. Initially, hydrolysis of the three labile groups occurs. Condensation to oligomers follows. The oligomers then hydrogen bond with OH groups of the substrate. Finally, during drying or curing, a covalent linkage is formed with the substrate with loss of water. Although described sequentially, these reactions can occur simultaneously after the initial hydrolysis step. At the interface, there is usually only one bond from each silicon of the organosilane to the substrate surface. The two remaining silanol groups are present either in condensed or free form ([Figure 5.26](#)).

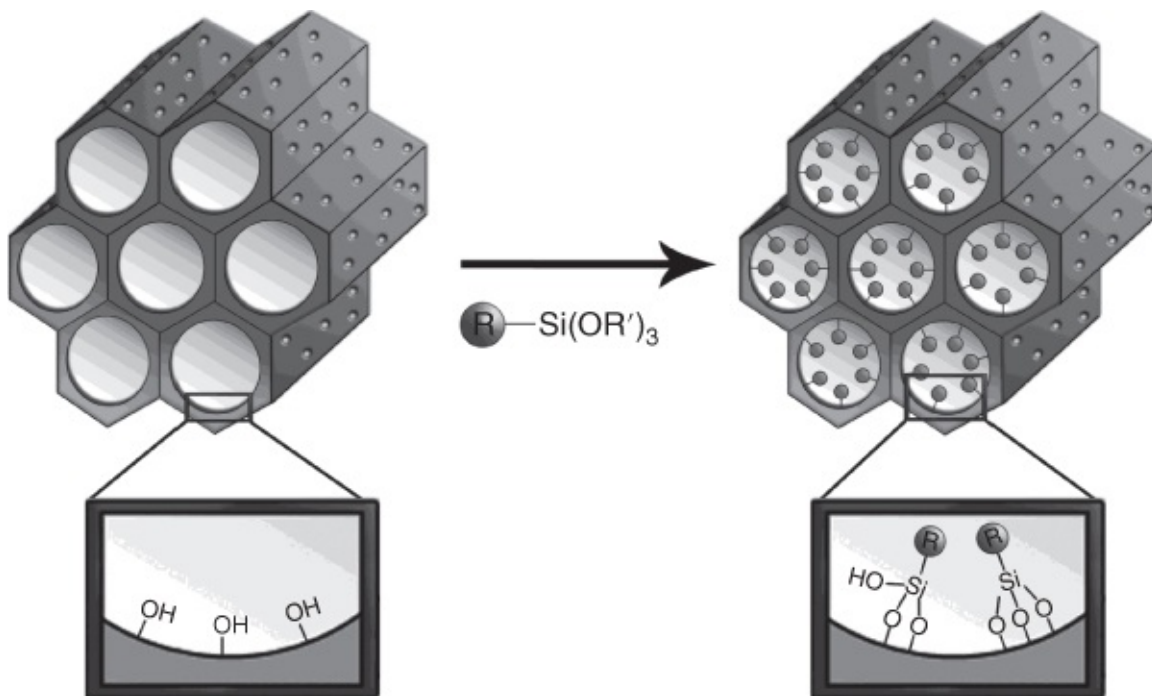


[Figure 5.26](#) Silylation of SBA-15.

Source: Figure is redrawn from Fröba's excellent review [35], Reproduced with permission of John Wiley & Sons, Ltd.

Van Der Voort gave a nice example of the combination of both techniques back in 1999 [37]. First, a silica surface was functionalized with a chlorosilane (dimethyl dichloro silane) to remove the surface silanols and to render the surface much more hydrophobic by the methylsilyl groups (species A in [Figure 5.27](#)). As new SiCl functionalities are created, these groups can be easily hydrolyzed (just by ambient air) and this “second generation” isolated silanols are then reacted with an active organometallic complex, vanadyl acetylacetonate, or $\text{VO}(\text{acac})_2$ (species B). Finally, a calcination step removes the organic ligands, and a dihydroxyvanadyl species is grafted on the silica surface (species C). This species is surrounded by a hydrophobic environment and cannot “surf” on the surface. Vanadium oxide species on silica are very mobile and move rapidly on the silica surface, until they coalesce into large clusters and crystals of V_2O_5 . This mechanism is prohibited here, and in fact, one of the first “single site catalysts” was created, long before the term gained widespread popularity.

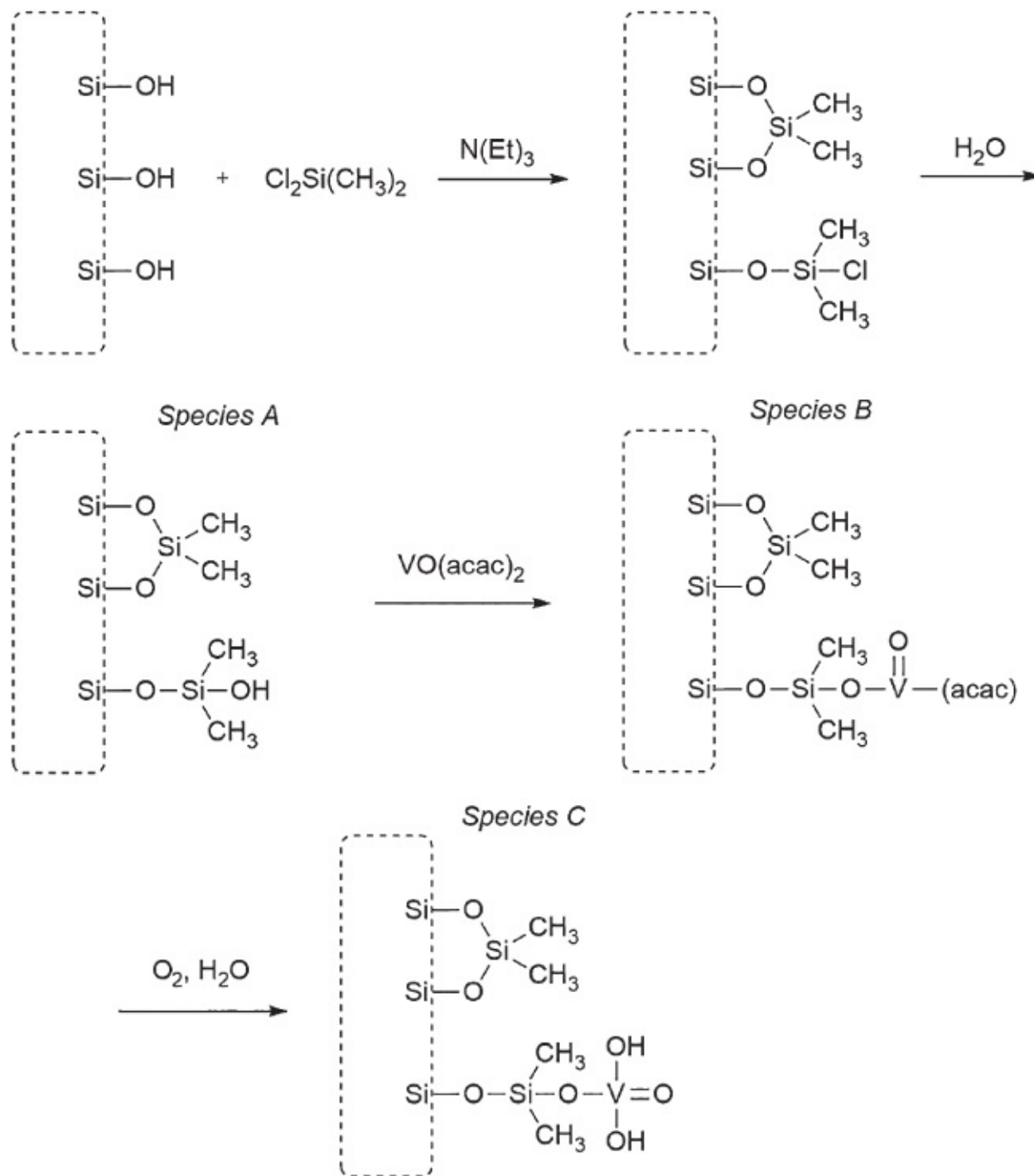


Figure 5.27 Creating isolated and stable vanadyl groups on silica by silylation.

Source: Redrawn and reproduced with permission of ACS [37].

5.2.1.1.5 Gas Phase Coating Techniques – Atomic Layer Deposition (ALD)

Coating techniques can be defined as all procedures that share the final aim of creating a thin layer on a foreign substrate. The thickness of such a coating varies from a monomolecular layer to several millimeters. The most conventional technique is Chemical Vapor Deposition (CVD) and its variants (Metal-Organic CVD [MO-CVD], Plasma Enhanced CVD [PE-CVD], and Laser CVD [L-CVD]). However, these techniques are not often used to coat mesoporous silica powders, they are typically used in the fields of microelectronics and

photonics, mostly on well-defined flat surfaces (silicon wafers).

We will therefore only discuss the technique of ALD. Although also originally developed to create lighting panels (information boards in airports, etc.), the technique has evolved to an advanced technique to create catalysts.

CVD involves a very complex mixture of gases and/or ions, causing numerous uncontrollable side reactions. From a chemical point of view, these reactions are extremely difficult to monitor.

This was recognized by Suntola in the 1980s when he developed a new coating technique: Atomic Layer Epitaxy (ALE) [38]. ALE is a method for producing thin films and layers of single crystals one atomic layer at a time, utilizing a self-control obtained through saturating surface reactions. ALE is based on separate surface reactions between the growing surface and each of the components of the compound, one at a time. These components are supplied in the vapor phase, either as elemental vapors or as volatile compounds of the elements.

Note

On the other side of the “iron curtain” in those days, A.A. Malygin was building a very similar approach, it was called Molecular Layering. Due to the political situation in those days, the term Molecular Layering never really broke through in the West, as most publications were in Russian. An English publication [39] has appeared in the framework of NATO's Science for Peace Program.

ALE was originally developed to meet the needs of improved ZnS thin films and dielectric thin films for electroluminescent thin film display devices. However, soon it became clear that any combination of a very reactive metal complex, followed by pulse of a second gas (usually water, ammonia, H_2S), can create any sort of thin layer. So, it was picked up again later under the name ALD. Epitaxy means crystalline overgrowth, for catalysis the layers do not have to be epitaxial, so a more general “deposition” was used. The main advantage of ALD is therefore that the layers are built up “layer by layer” (LbL) allowing fine control over the thickness of the layers. The general principle of ALD is visualized in [Figure 5.28](#) and an example on how to make an alumina thin layer is shown in [Scheme 5.28](#).

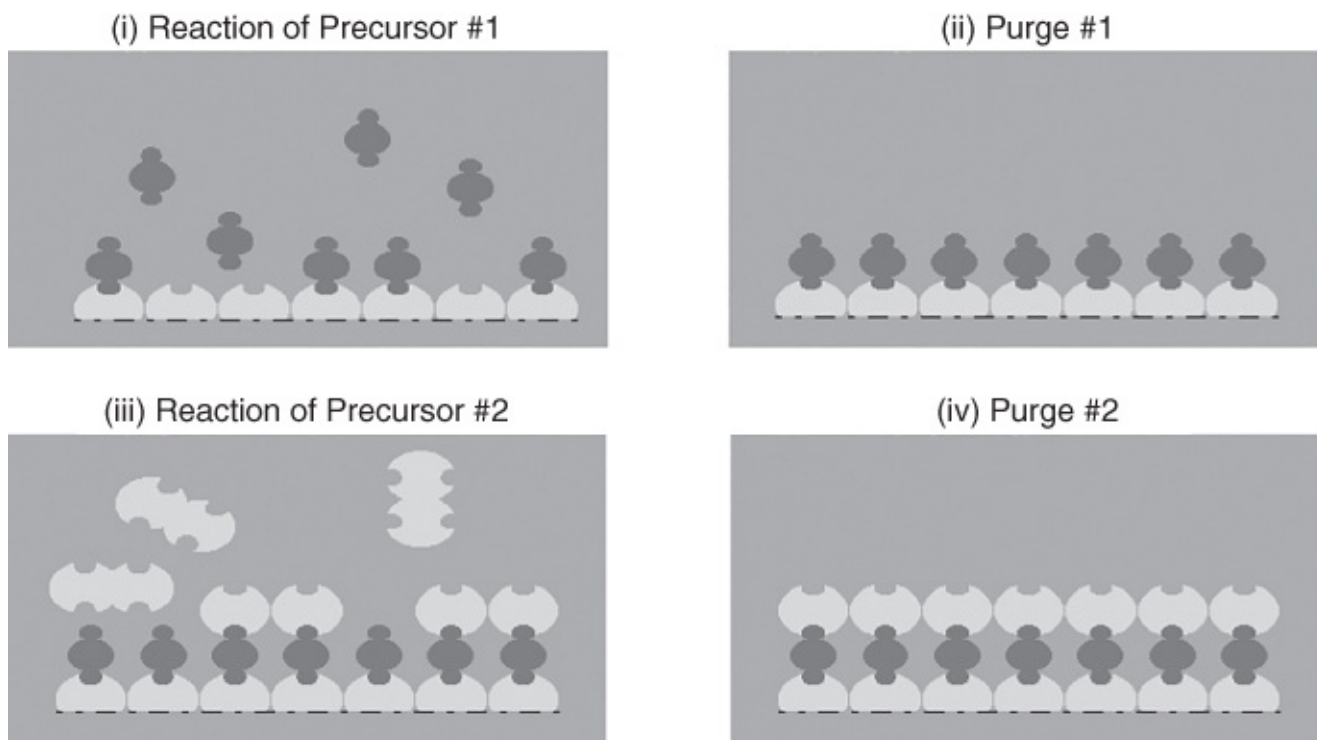
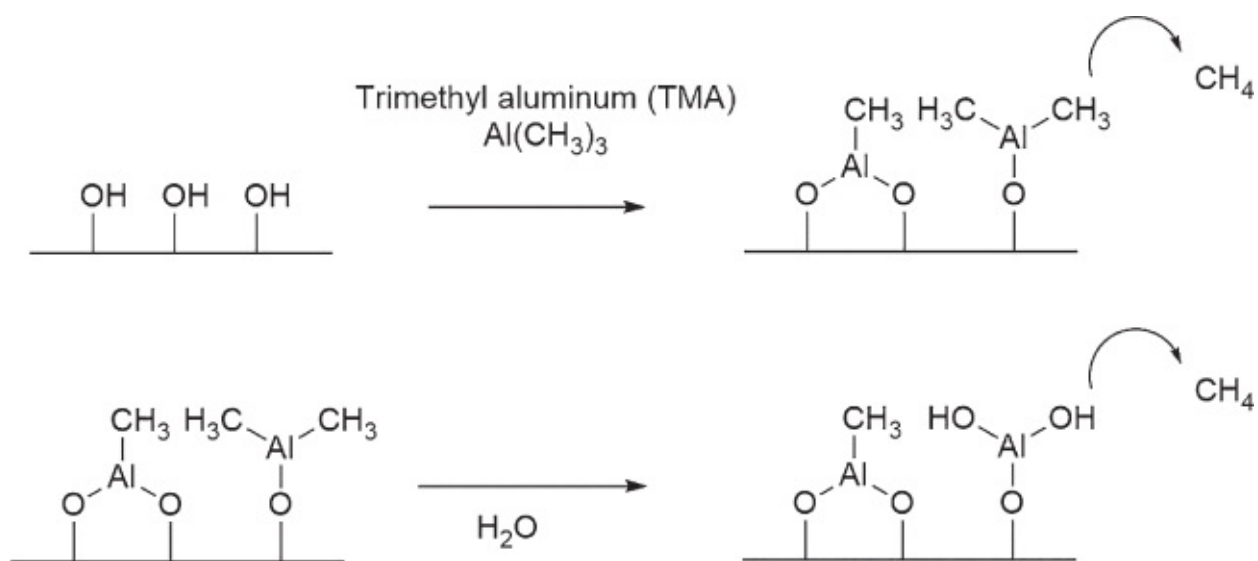


Figure 5.28 ALD Process, (i) a pulse of the first reactant is introduced; (ii) reactant 1 reacts until the surface is covered with exactly one monolayer after which residual molecules are pumped off; (iii) a pulse of reactant 2 is introduced, reactant 2 must react with reactant 1; (iv) reactant 2 forms a monolayer on top of reactant 1.



Scheme 5.3 ALD process for one monolayer of Al_2O_3 : Trimethyl aluminum, reacts with the silanols with release of CH_4 ; as a second reactant water is introduced creating Al-OH sites, again with release of CH_4 . A second cycle would start again with TMA, reacting again with the Al-OH sites. The layer forms “atom per atom” on the surface.

Research on ALD is still emerging in the field of catalysis. In a recent study, Van Der Voort has shown the amount of fine-tuning that is possible by ALD [40] (see [Figure 5.29](#)). By deposition of HfO_2 on an inkbottle type titania (compared to a planar substrate), one can

clearly observe the narrowing of the pores that occurs linearly until the pore mouth becomes too narrow to allow the metal complexes, after which the pore is sealed, but is still not completely filled. This was confirmed by sorption experiments, we created “closed but unfilled” pores.

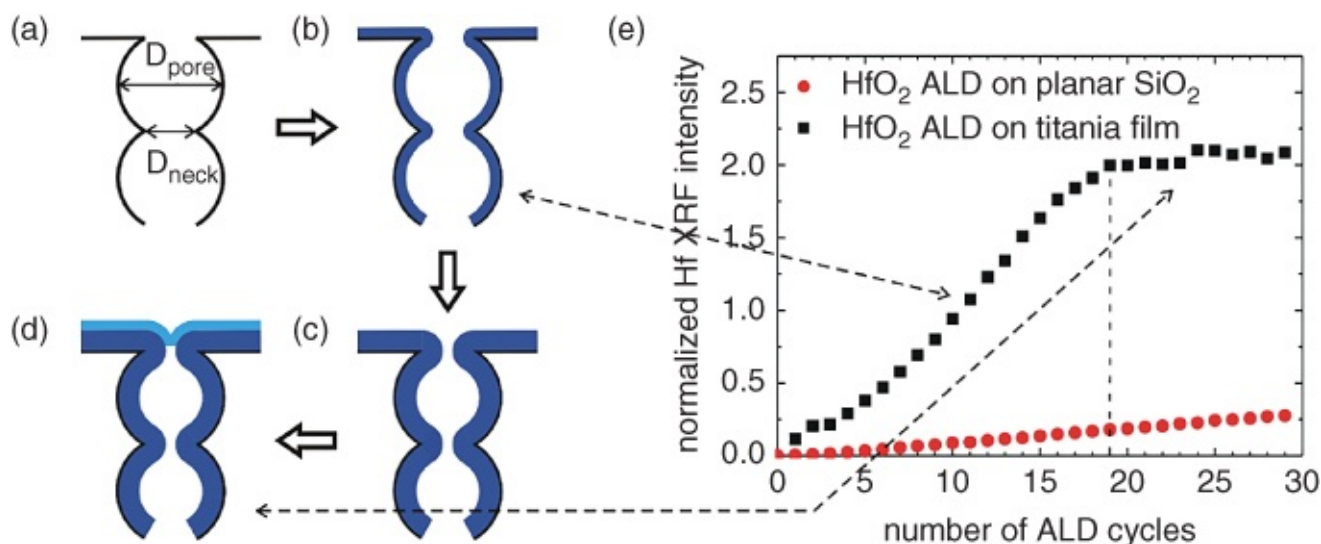


Figure 5.29 ALD of HfO_2 on an inkbottle titania pore.

5.2.1.2 Functionalized Mesoporous Silica in Heterogeneous Catalysis

Silica (as gel or aerogels) are often used supports for heterogeneous catalysts. So, all the reactions that apply to silica gels obviously also apply to ordered mesoporous silicas. The ordered materials offer the advantage of a much higher surface area (more active sites possible per gram material) and the ordered mesopores (offering improved diffusion and possible shape selectivity).

Silica as a support has a number of important disadvantages:

(1) The stability of the anchored groups on silica in humid air and water is relatively low. As we discussed in [Chapter 4](#), the siloxane bond is prone to hydrolysis; one siloxane bond (SiOSi) splits with water into two hydroxyl groups (SiOH HOSi). This not only reduces the structure of the entire silica structure over a period of time; even more importantly, the functional groups that are usually anchored with reaction with the silanols are equally prone to hydrolysis. This results in a complete loss of functional groups when the catalyst is used in moist conditions. Only water-free processes are suitable for long-term catalysis life. (Of course, as in Fluid Catalytic Cracking [FCC] where the catalyst is continuously refreshed, this might still be worthwhile in certain applications.)

(2) Typical “acid oxides,” with a low PZC (e.g. vanadium oxides, titanium oxides, tungsten oxides, chromium oxides, etc.) are highly mobile on the acid surface of silica. This means that even carefully grafted metal oxides as single sites are highly mobile. As soon as the reaction temperature increases, these species become much more mobile and will “skate” or “surf” on the silica surface and will cluster together toward first

nanosized clusters that eventually grow into large metal oxide clusters. A typical example is shown in [Table 5.5](#): Predicted surface VO_x species as a function of the acidity of the support. The very acid VO_x species (V_2O_5 has a PZC of 2) bond very strongly to the basic hydroxyl sites on the MgO surface and only the single site V species are observed. MgO is not always a good catalytic support, it has a very low surface area, is very soft (attrition), and dissolves in many solvents including water. When the PZC of the supports increases, the isolated V-sites do not longer form, and on the very acidic silica support mainly large clusters of V species are formed.

Strategies have been developed to avoid this, see for example earlier in this chapter on the hydrophobized silica surrounded VO_x species ([Figure 5.27](#)).

Table 5.5 Predicted surface VO_x species as a function of the acidity of the support.

Oxide support	pH of support (at PZC)	Predicted VO_x species
MgO	11	$\text{VO}_3(\text{OH})$
Al_2O_3	8.9	$\text{VO}_3(\text{OH})$
TiO_2	6.0–6.4	$\text{VO}_2(\text{OH})_2(\text{VO}_3)_n$
ZrO_2	5.9–6.1	$\text{VO}_2(\text{OH})_2(\text{VO}_3)_n$
Nb_2O_5	4.3	$\text{V}_{10}\text{O}_{27}(\text{OH})(\text{VO}_3)_n$
SiO_2	3.9	$\text{V}_2\text{O}_5\text{V}_{10}\text{O}_{26}(\text{OH})_2$

Let us see if the promised advantages (higher catalytic activity due to higher surface area and shape selectivity) have found some practical applications. Also, the larger pores can accommodate much larger catalytic groups, so larger organometallics can be loaded in the mesoporous silica pores as well.

5.2.1.2.1 Bifunctional Catalysts

We start with the anchoring of two functions at the same time. This would not work in the homogeneous phase because the active groups would react or interact with each other and get neutralized.

Huang et al. [41] published the following procedure in 2011 to synthesize bifunctional acid/base catalysts ([Figure 5.30](#)). Please note that this represents just one example out of hundreds of papers that have appeared on the synthesis of bifunctional mesoporous silica catalysts. By combining two silanes, being the regular TEOS and a mercaptopropyl trimethoxysilane (called STMOS by the authors) a mesoporous silica (in the form of nanoparticles) was synthesized using the classic synthesis with CTAB in basic media. This way, both silanes co-condense to form a mercapto-groups containing silica nanoparticles. These functional groups are inside the pore system of the nanoparticles. Subsequently, without removing the surfactant, these particles are treated with an amine containing silane,

aminopropyl trimethoxysilane (called APTMOS by the authors) in dry toluene. As the pores are still completely filled by the CTAB surfactant, the APTMOS can only react on the outer surface of the nanoparticles, creating aminopropyl functional groups on the particles. In the final step, several things occur simultaneously: the thiol (mercapto) groups are easily oxidized by H_2O_2 , the surfactant is washed out, and the material is dried under vacuum at $150\text{ }^\circ\text{C}$. The final product is a bifunctional catalyst with strong acidic groups in the pores and mild basic groups on the outside of the particles ([Figure 5.30](#)).

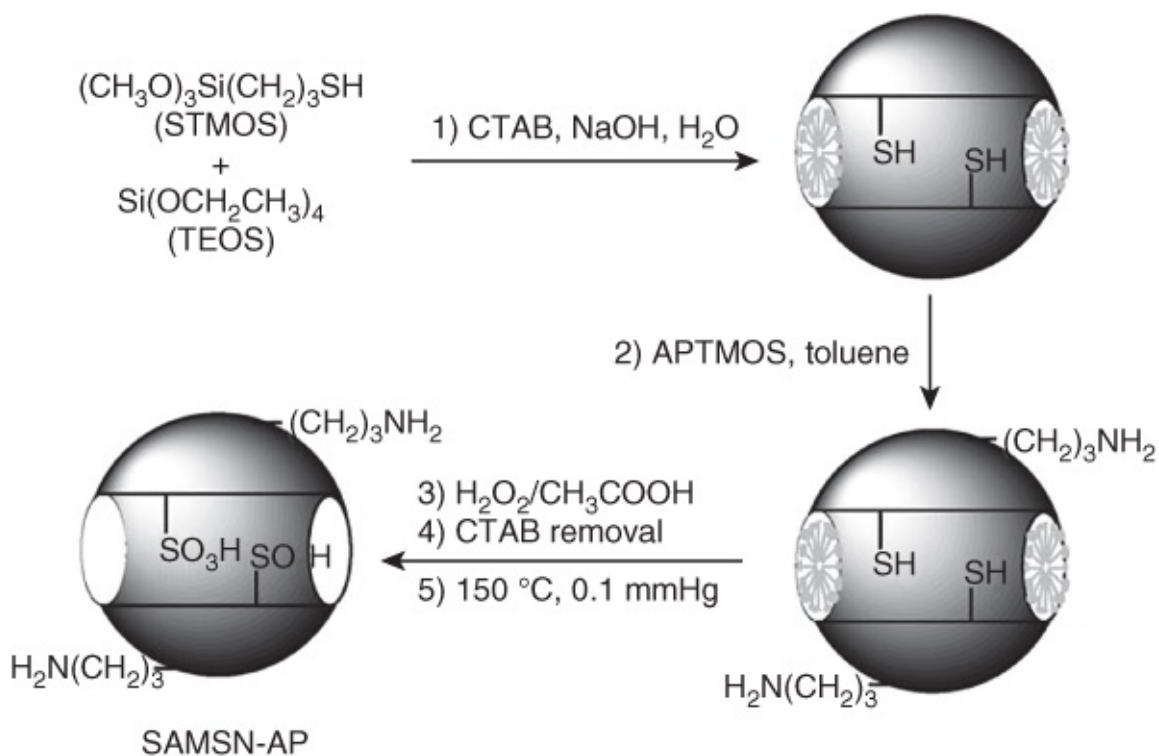


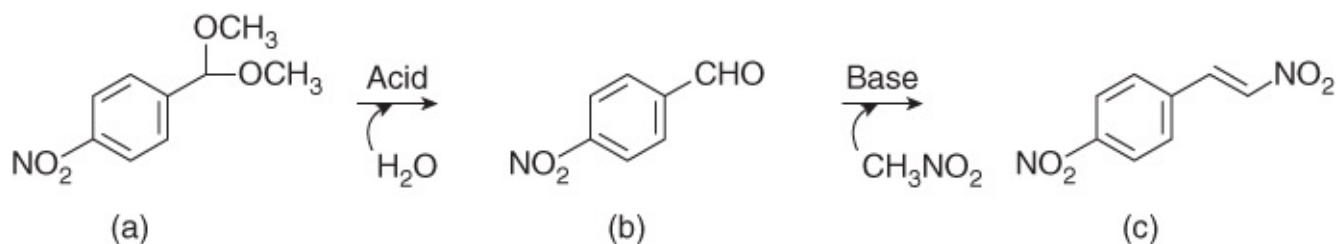
Figure 5.30 Synthesis of a bifunctional acid/base catalyst according to Huang.

Source: Reproduced with permission of John Wiley & Sons, Ltd [\[41\]](#).

Authors subsequently tested this bifunctional catalyst in a *cascade reaction*. A cascade reaction is a reaction that normally requires two different catalysts after each other. The authors chose a cascade of an acid-catalyzed hydrolysis of an acetal (product A in [Table 5.6](#)) toward an aldehyde (product B). This step is acid catalyzed only. The following reaction, the Henry reaction, is strictly base catalyzed and yields the end product (C). The entire reaction is shown in [Scheme 5.30](#).

Table 5.6 One-pot reaction cascades composed of acid-catalyzed hydrolysis and base-catalyzed Henry reaction.

Entry	Catalyst	B (%)	C (%)	Conv. of A (%)
1	SAMSN-AP	2.3	97.7	100
2	SAMSN/APMSN	4.5	95.5	100
3	SAMSN	100	0	100
4	APMSN	0	0	0



Scheme 5.4 Reaction conditions: Catalyst A: (100.0 mg, 1.5 mmol), H₂O (1.5 mmol) CH₃NO₂ (1.0 ml), 80 °C, 48 h. Conversion and yields were determined using GC data. AP: 1-aminopropane, PTSA: *p*-toluenesulfonic acid.

When the authors used the bifunctional catalyst (see [Table 5.6](#)), they called it SAMSN-AP, it is clear that the cascade reaction goes to completion, yielding 100% conversion, and 97.7% yield of the end product. Some intermediate product is still left, but this should be no problem for the synthesis of C.

The authors also tested – and this is commendable – a 50/50 mixture of nanoparticles only functionalized with amino groups and only functionalized with sulfonic acid groups. This resulted in almost the same product distribution (entry 2 in [Table 5.6](#)).

Using only the acid catalyst, 100% of A is converted to 100% B, but B does not react further, as could be expected (entry 3).

Finally, using only the base catalyst, nothing happens at all, as the starting product A cannot be converted by a base catalyst (entry 4).

5.2.1.2.2 Accommodating Large Organometallic Complexes

The large pore diameter of mesoporous silicas is able to accommodate much larger catalytic functions than that the zeolites or zeotypes. Organometallic catalysts are known to be very reactive and selective and won the Nobel Prize for Chemistry not so long ago. They are usually very expensive, not as much compared to the costs of the expensive noble metals (Pd, Pt, Au, Ag, Ru, Ir, ...) but more importantly by the costs of the sometimes very expensive ligands.



Photo: U. Montan
Yves Chauvin
Prize share: 1/3



Photo: R. Paz
Robert H. Grubbs
Prize share: 1/3

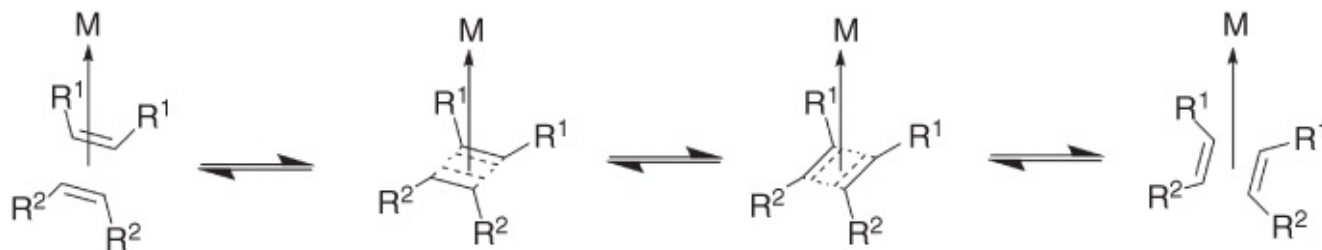


Photo: L.B. Hetherington
Richard R. Schrock
Prize share: 1/3

The Nobel Prize for Chemistry was in 2005 awarded to three scientists: Chauvin, Grubbs, and Schrock. All three scientists had independently developed important catalysts for the metathesis of olefins, a very important chemical reaction. Metathesis is ancient Greek for “changing position.”

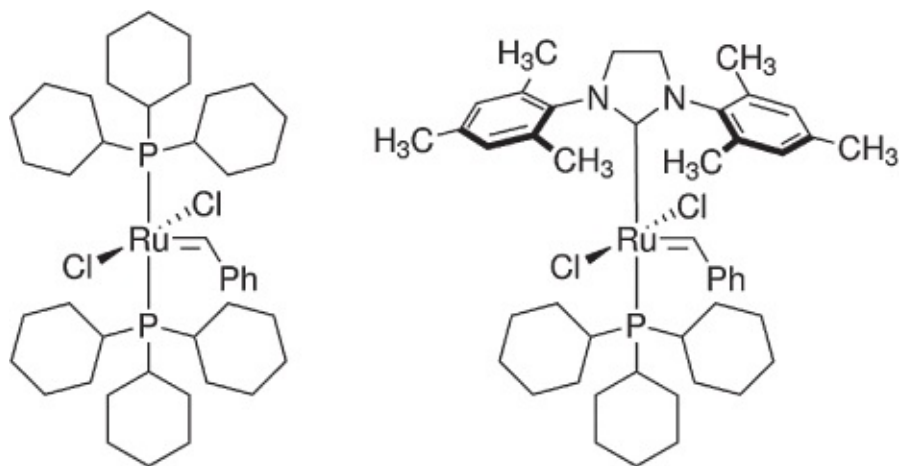
(Photo: <https://www.nobelprize.org/prizes/chemistry/>).

The metal catalyzed olefin metathesis roughly follows [Scheme 5.30](#):



[Scheme 5.5](#) Metal catalyzed olefin metathesis.

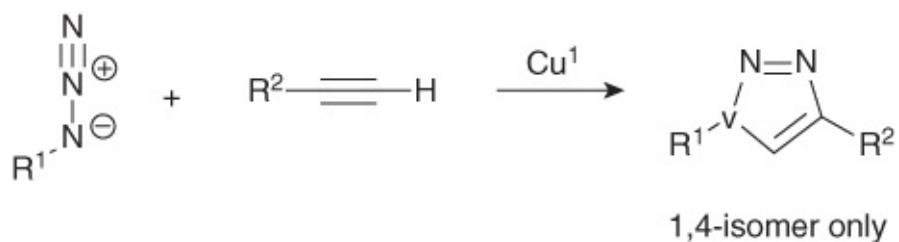
However, the ligands that are coordinated to the metal site are crucially important. As an example, we show the Grubbs first and second generation catalysts that are commercially available now. They come at a price though. Checked on January 4, 2018 at the site of a very large commercial supplier, 10 g of Grubbs second generation catalyst costs €1805 or about USD\$ 2175. Normally, these catalysts get lost during the reaction. So, next to the loss of expensive catalyst, and especially in the pharmaceutical industry, an even more expensive purification step is required to remove the toxic catalyst from the end product. For this reason, the heterogenization of such a catalyst on a porous support would be highly interesting and beneficial. The big questions are however: (i) Is the heterogeneous catalyst still active enough? (ii) Is there no leaching of toxic materials out of the heterogeneous catalyst? (iii) Is the catalyst easily recyclable? (iv) Is the recycled catalyst still active for another run? Finally, (v) What is the lifetime of the catalyst? ([Scheme 5.30](#)).



[Scheme 5.6](#) Grubb's first- and second-generation catalyst.

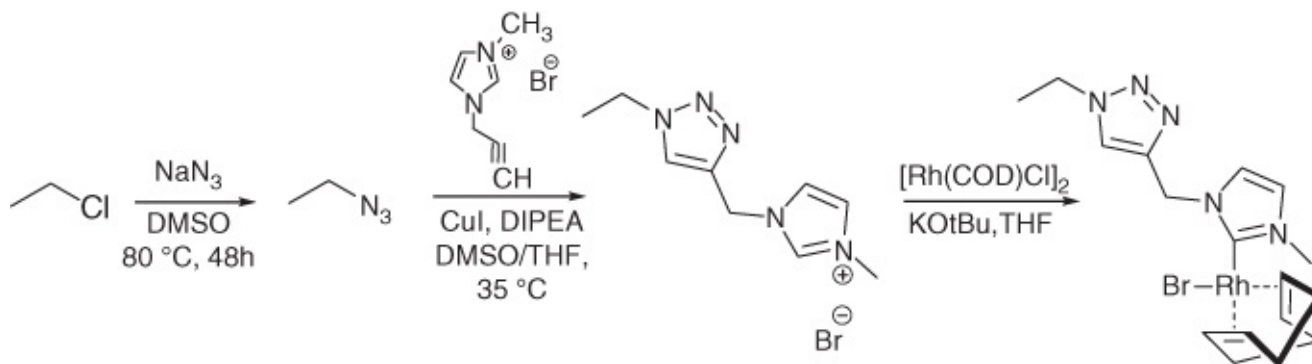
In a very recent and lengthy review in *Chemical Reviews*, Kühn and coworkers [42] discussed all possible strategies and applications. We just show one of the many methods that uses the convenient *click chemistry*. It is not about the Grubbs catalysts, but a very similar metal complex. We will discuss the advantages of click chemistry further in the next chapter on PMO materials.

Although Cai and He [43] reported this procedure for a Merrifield resin, the procedure would also be valid for a mesoporous silica. In that case, a chlorosilylated mesoporous silica is exchanged with N_3^- functions. The group performs a simple click reaction by use of a Cu(I) catalyst, known as the CuAAC click reaction, with the general [Scheme 5.30](#).



[Scheme 5.7](#) Copper mediated click reaction.

So, adding 3-methyl 1-propargylimidazolium bromide to the azide functionalize silica yields easily, by the aforementioned click reaction compound (3). Finally, adding the $[\text{Rh}(\text{COD})\text{Cl}_2]$ yields the final heterogeneous catalysts. The catalyst had excellent properties and was fully recyclable. Using click chemistry, these catalysts can be easily prepared. Hundreds of other examples in the synthesis of heterogeneous catalysts based on mesoporous silicas can be found in the review that we mentioned earlier [42]. In this book, we will explore another type of click reaction (thiol-ene click reaction) in great detail in the chapter on PMOs ([Scheme 5.30](#)).



Scheme 5.8 Synthesis of a heterogeneous organometallic catalyst.

Source: Redrawn from ref. [43] with permission.

5.2.2 In Adsorption

5.2.2.1 Sorption of Metal Species

One of the earliest applications of mesoporous silicas was the adsorption of heavy metal ion (toxic ions) in water. Due to the large surface area and mesopores, the silica can be functionalized with metal attracting functional groups. The Soft and Hard Acid and Bases theory by Pearson is an easy starting point. The heavy metals, such as mercury and lead, bond preferably to soft ligands. Two very good soft ligands are amines and thiols.

Pinnavaia and coworkers [44] showed how thiol modified mesoporous silica easily captures Hg-ions, with little competition from typical concurring ions, such as Cd-ions, Pb-ions, and Zn-ions. The selectivity of the adsorbent is just as important as the capacity of the adsorbent. Usually, the targeted ions are present in a much lower concentration than the competing ions (think about Na^+ , K^+ , NH_4^+ ions...) or even other soft ions. It is of paramount importance that only the targeted ions are captured. The materials were easily synthesized by reaction the mesoporous silica with mercaptopropyltriethoxysilane.

We will return more extensively on the sorption of metal ions in aqueous media in the following chapters.

5.2.2.2 Chromatography

Out of all applications domains for mesoporous silica particles, we believe the chromatography is the highest commercialized at the moment, as many columns can be purchased that contain porous silica particles. You will notice that – contrary to most other sections – most references originate in this section from patent literature.

The performance of chromatographic columns is strongly influenced by particle design. Uniform particles allow for a more homogeneous packing of a column and reduce the *Eddy diffusion* through the column, which leads to reduced peak dispersion. Since chromatography is in essence a diffusion-controlled process, the architecture of the pores in the material plays an important role in both the efficiency and the retention experienced with a particular type of packing material in a column. Current silica based stationary phases exhibit a broad pore

size distribution. This means that no two pathways throughout the particle are identical and that not every functional group is equally accessible (see [Figure 5.31](#)).

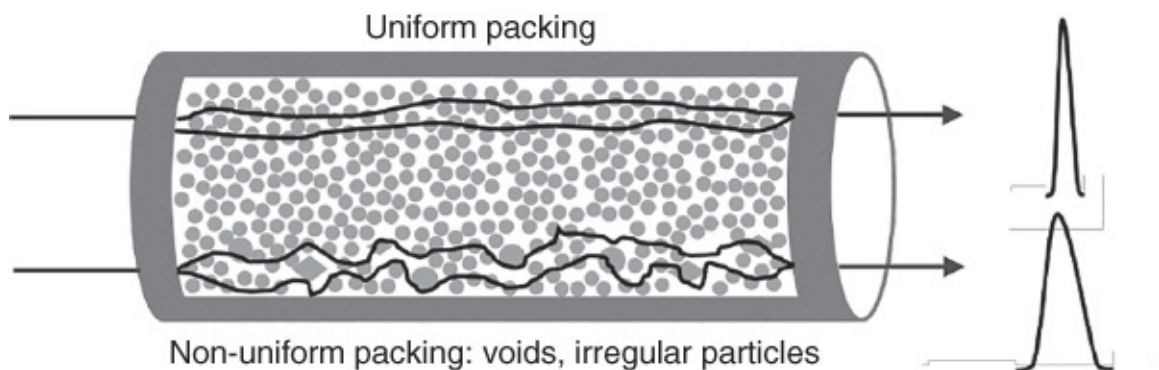


[Figure 5.31](#) Graphical representation of the Eddy diffusion term throughout a column. Uniform pathways result in narrow peaks (top), poor quality of the column causes peak broadening (bottom).

To reduce diffusion times through the particle, superficially porous particles were introduced. Superficially porous particles successfully improve the chromatographic performance. However, inherent to this particle design a reduced phase ratio leads to a lower sample loadability and a reduced retention. To deal with this drawback an ordered pore system with a strongly increased surface area could offer a solution.

We will not discuss the fundamentals of chromatography here. The interested reader is referred to some excellent books on this topic [[45](#)].

The Achilles heel of HPLC still is the hydrolysis of silica. Due to this susceptibility of silica materials to hydrolysis, conventional column performance is easily affected when using harsh conditions such as elevated pH or higher temperatures in combination with a highly aqueous mobile phase. This instability of silica packing materials is reflected in a reduced column efficiency and a reduced retention as a function of the number of chromatographic runs.

Endcapping of the silanols was the first solution and more recently researchers started to add more carbon to the stationary phase with semi and full hybrid types of silica, even fully carbonated stationary phases were tried.

Ordered mesoporous silica particles offer the advantage of uniform pore sizes and enhanced surface areas. The famous group of Klaus Unger [[46](#)], well known silica specialist and chromatographer, in collaboration with Ferdi Schüth, compared already back in 1996 the then “novel” MCM-41 particles with commercial materials, including the LiChrosphere Si 100 (actually a fumed silica or an aerosol, see [Chapter 4](#)). As no protocols to produce spherical mesoporous silicas were in place yet, these particles were just grinded to proper dimensions and irregular in shape. In this experiment, the LiChrosphere particles outperformed the MCM-41, proving again the importance of monodispersed spheres for chromatography.

It became clear that uniform and spherical particles are extremely important for a good

separation. The characteristics of an “ideal” chromatographic particles are summarized as follows:

- Particles should be spherical.
- Particles should be monodisperse, $D_{90/10} < 1.6$.¹
- Particles must be between 2 and 5 μm diameter for analytical purposes and between 5 and 15 μm for preparative purposes.
- Surface area should be high, at least higher than $50 \text{ m}^2 \text{ g}^{-1}$, but much higher is better.
- Pore size should be large in the mesopore range, diameter should be larger than 6 nm.
- There should be as little micropores as possible, $S_{\mu}/S_{\text{BET}} < 0.1$.
- Mechanical stability should resist the harsh packing and analysis pressures.
- Particles should be hydrolytically stable between below $\text{pH} = 2$ and above $\text{pH} = 12$.
- Particles should be stable at temperatures above $100 \text{ }^\circ\text{C}$.
- There should be no (metal) impurities.

5.2.2.3 Methods to Synthesize Spherical Mesoporous Particles

5.2.2.3.1 Fully Porous Spherical Particles

Monodisperse silica particles were first described by Stöber in 1968, who performed the hydrolysis and condensation of TEOS in water using ethanol as a dispersing co-solvent and ammonia as the catalyst [47]. This delivered, depending on the reaction conditions, solid particles with a controllable size between 50 and 2000 nm. Based on this groundbreaking invention, multiple pathways toward porous particles have been developed. In the first approach, these solid nanoparticles are fused in a controlled way to form a spherical particle with mesoporous voids between the original nanoparticles. This is done by *coacervation*, a technique where silica nanoparticles are brought together during a polymerization reaction. As described by Destefano and Kirkland [48], the silica nanoparticles are mixed with monomers of melamine or urea and formaldehyde. As polymerization takes place, the nanoparticles co-precipitate and after removal of the polymer by calcination, uniform micron-sized spheres are found (see [Figure 5.32](#)).

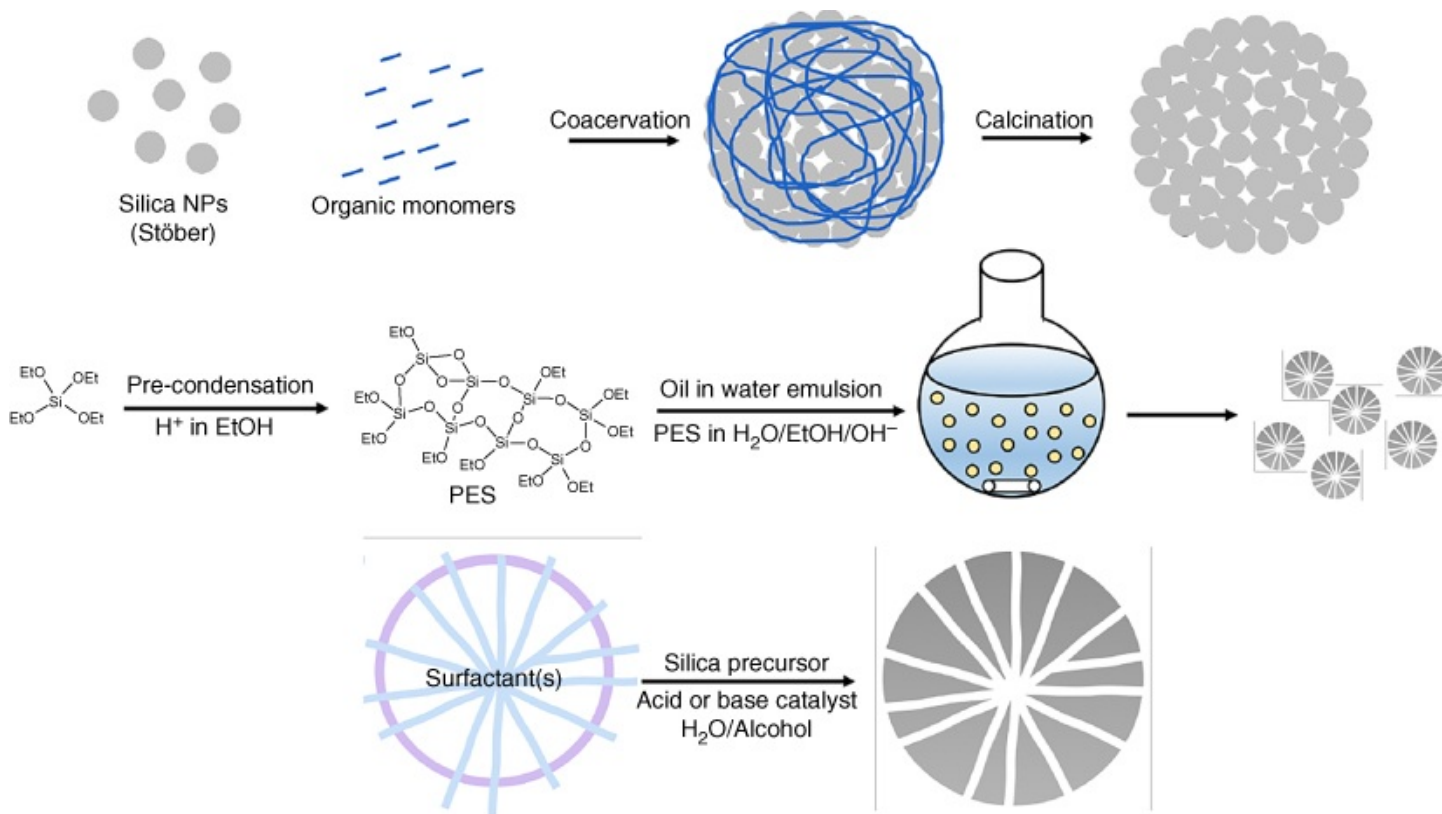


Figure 5.32 Graphical representation of the coacervation method (top), the Unger method (middle), and the adapted Stöber method (bottom) to obtain fully porous silica spheres.

Secondly, Unger and Schick–Kalb developed a Stöber-like method in 1971, where pre-condensed TEOS, that is, poly(ethoxysiloxane) or PES, is used as starting point instead of a silica sol [49]. This PES is subsequently emulsified in a water/ethanol mixture in which it forms microdroplets. Addition of a base catalyst starts hydrolysis of the PES, which results in the formation of porous beads. The condensation degree, measured by the viscosity of the PES, is claimed to control porosity, while the particle size is controlled by the stirring speed.

A third, similar option is to take the original Stöber method and add pore generating surfactants as described by Unger's group in 1997 [50]. Depending on the surfactant, pore size and ordering can be controlled, however, it seems more practical to expand smaller pores with a post-synthetic hydrothermal treatment. This approach has further been investigated by other groups, who managed to produce spheres in an acidic medium by using hydrochloric acid as a catalyst. The properties of the particles remained roughly the same except these could reach diameters up to 1 mm [51]. As a main benefit for this templated method, highly monodisperse particles are obtained that do not require physical separation by means of classification.

In 1998, another synthesis pathway for mesoporous silica spheres was introduced by Qi et al. [52]. A mixture of CTAB and the non-ionic surfactant Brij-56 combined with TEOS as silica source was used for liquid-crystal templating under acidic conditions but without the addition of a co-solvent. The resulting particles reveal a particle diameter of 2–6 μm and all characteristic properties of the ordered mesoporous materials.

Copyright © 2019, John Wiley & Sons, Incorporated. All rights reserved.

Next to this, spherical particles of porous silica can also be obtained by employing water-in-oil emulsions [53] or by spray drying [54]. Both processes essentially create droplets in which xerogel particles form. Inside these spherical microdroplets, the porosity can be controlled, either by the sol-gel process occurring inside or by adding surfactants. Herein, quality of the droplet is of primordial importance as this controls the size and dispersion of the particles. With these colloid methods, it is easy to increase the particle size above those obtained in Stöber-type syntheses, while control of particle size and pore size is effectively decoupled. However, with spray drying, it does not seem trivial to obtain monodisperse particles in the size range applicable for HPLC. Furthermore, considering particles with ordered porosity, an evaporating solvent (EtOH) needs to be used together with a pore generating surfactant in order to obtain porous particles. Due to these constraints, it remains challenging to obtain large mesopores via spray drying.

Finally, another interesting procedure is called *pseudomorphic transformation*. This method, described by Anne Galarneau, highly resembles a redeposition/pore etching process that is often used to enhance the porosity of mesoporous silica particles, but now involves the addition of a surfactant, or SDA. The process starts from commercial porous silica particles. Stirring these particles in an alkaline solution (NaOH), water, and CTAB at elevated temperatures partly dissolves the particle. However, redeposition of this dissolved silica is believed to occur around the surfactant. As a result, ordered MCM-41 type pores are obtained (CTAB inducing a pore size of approximately 4 nm), while the spherical morphology is maintained. Later MCM-48 type materials were developed via this method (see [Figure 5.33](#)) [55].

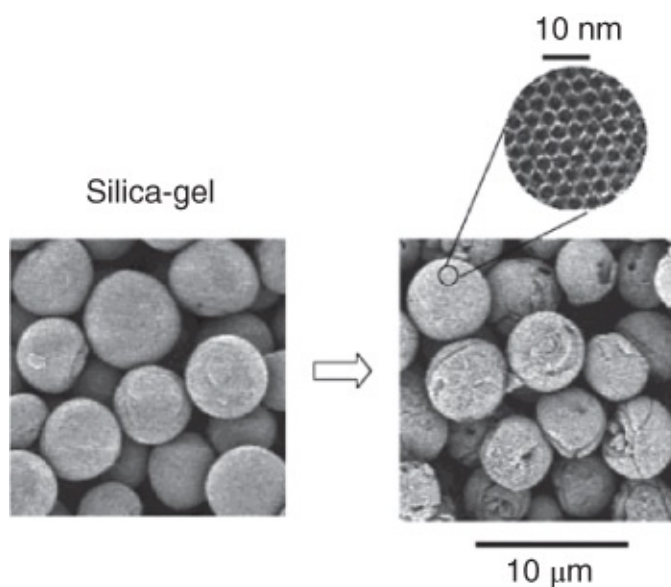


[Figure 5.33](#) SEM images of Nucleosil 100-5 before and after its pseudomorphic transformation into as material with ordered pores (MCM-41).

Source: Reproduced with permission of ACS [55].

Commercially, many columns packed with fully porous silica particles, both pure and modified, are available.

5.2.2.3.2 Core-Shell Particles

Core-shell or superficially porous particles were envisaged by Horvath and Lipsky [56] as early as 1969 and subsequently developed by Kirkland [57] (Figure 6.22). These particles were prepared by coating a glass bead with poly(diethylaminoethylmethacrylate)acetate. Thereafter, 200 nm silica nanoparticles, as prepared by Stöber, are added at pH 3.6.

Coulombic attraction between silica and polymer causes a layer of nanoparticles to stick on the surface of the glass bead. After four growth rounds and a sintering step, this resulted in a stable core-shell particle. These materials were commercialized as Zipax[®] and investigated as supports for the now abandoned technique of liquid–liquid chromatography.

Bad results in the application, combined with a large particle size and ongoing advantages in fully porous particles, caused reduced interest in core-shell particles for many years.

Core-shell particles were revisited in 1992, again by Kirkland, who developed a technique using simultaneously spray drying of a mixture of large solid silica particles, obtained after sintering of monodisperse fully porous Zorbax particles, together with a sol of silica NPs [58]. The average size of the latter was 44 nm and resulted in a wide pore size distribution from 10 to 60 nm. Both this and the presence of fully porous aggregates, which were hard to separate, limited the use of these pioneering Poroshell[®] particles.

A major improvement was found in using a coacervation method as described earlier for fully porous particles, but using a large core particle or using a polyelectrolyte during the coating process [59]. Optimization of these methods has at least led to several commercial materials,

The Unger group, followed by others, developed another popular LbL growing approach that employs a template surfactant to grow a porous shell on top of a silica core [60]. After one synthesis round generally, a very thin 60–75 nm layer is grown with small pore sizes. However, when suitable templates are used and pore swellers are employed one is able to boost the pore size.

Wei introduced another possible method that starts from a solid silica particle with a mean size of 3.1 μm . The selective etching of the particle's surface now generates superficially porous particles [61]. An overview of the different methods is presented in Figure 5.34.

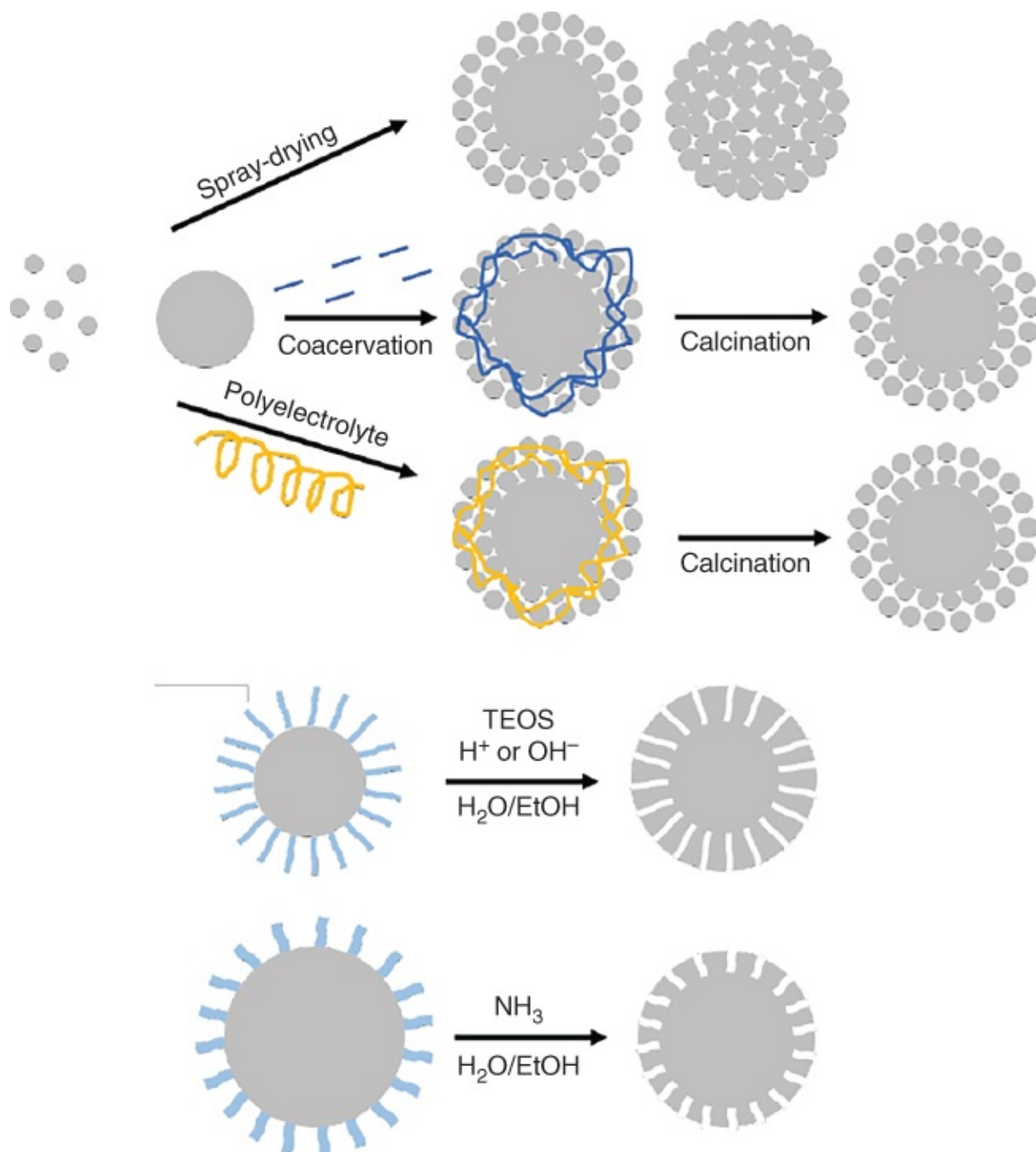


Figure 5.34 Graphic representation of synthesis methods to obtain core-shell type particles. Top: The methods of Kirkland using mixtures of large and small solid silica particles. Middle: The Unger and Eiroshell method applying surfactants to grow porous layers on top of a solid particle. Bottom: The Wei method taking advantage of selective etching in the presence of surfactants.

5.2.3 As a Drug Carrier

Mesoporous ordered silica, due to its large and uniform pores and its biocompatibility is ideally suited to adsorb biomolecules. A next step would be the controlled release of the biomolecules, this is usually called *controlled drug release*.

Especially for cancer chemotherapy, very toxic drugs are introduced in the body that are very damaging to the good cells as well. Researchers have been studying for decades ways to introduce the drugs at the location of the cancer cells only. The ideal transport vehicle would be a *smart material*, that responds to an *external trigger* (light, pH, heat, ...). If one would be able to introduce the drug in a mesoporous silica and close the pores, this would travel innocently in the body until a trigger “opens” the pores and the drug are slowly released at the desired location.

In a very recent review, Zhu et al. describe the recent progress in this field extensively [62]. We will limit our contribution here to a few illustrative examples.

Single stimulus responsive drug delivery systems are materials that release their encapsulated drugs upon one stimulus only. The stimuli are either pH, redox potential, enzyme interaction, light, temperature, magnetism, or ultrasound. For cancer treatment, the pH and the redox responsive systems are especially important, as cancer cells typically have a lower pH than healthy cells and contain a high concentration of GSH (glutathione, L- γ -glutamyl-L-cysteinyl-glycine, an active redox component).

The extracellular pH of most tumor tissues is more acidic (pH = 6.5–6.8) than normal tissues (pH = 7.4) due to the so-called Warburg effect. Moreover, the pH in the endocytic vesicle drops to 5.5–6.0 in the endosomes and to 4.5–5.0 in the lysosomes. So, pH-sensitive molecules can be used as “gate keeper” to keep the pores with the drugs inside closed until a low pH is encountered. Typical chemical gatekeepers, stable in neutral and basic media, but unstable in acid media are acetals, amines, boronates, and hydrozones (Figure 5.35a).

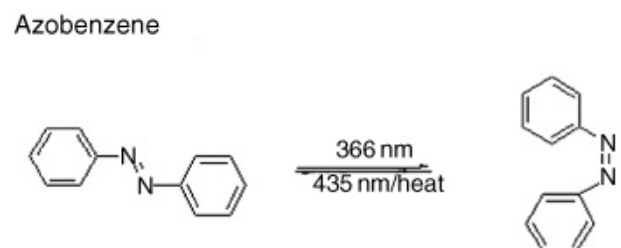
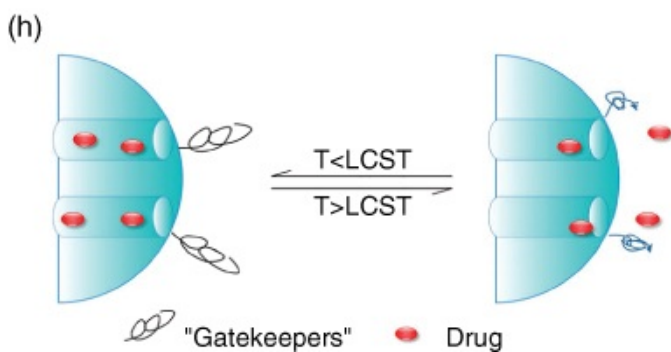
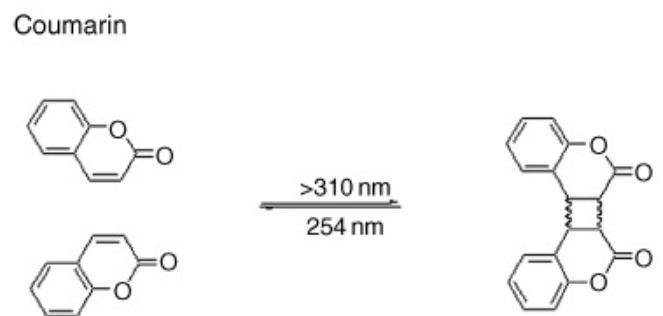
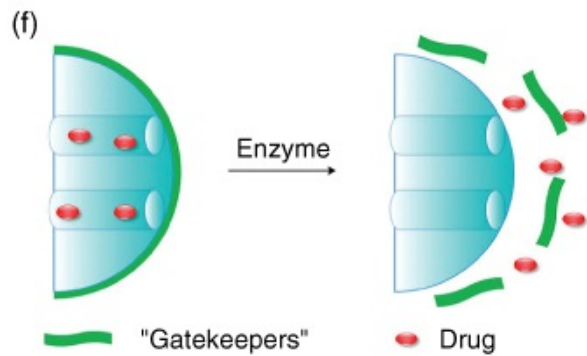
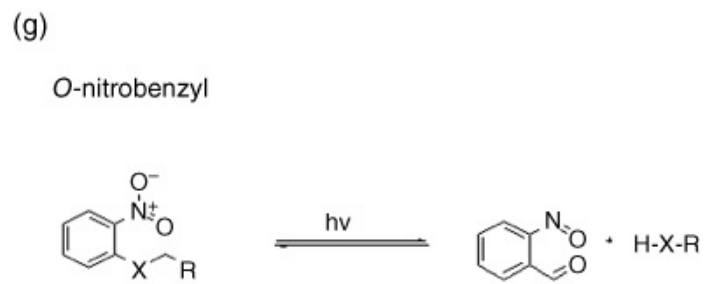
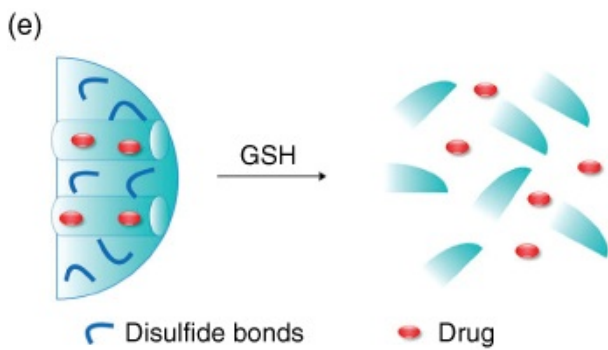
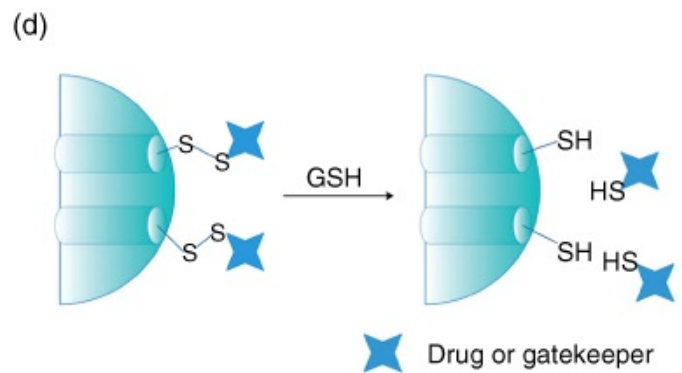
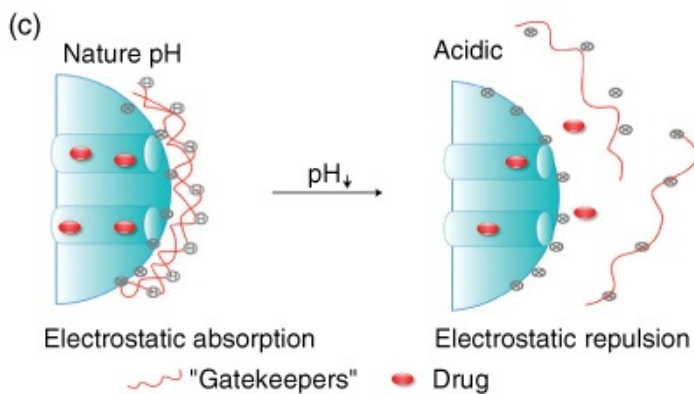
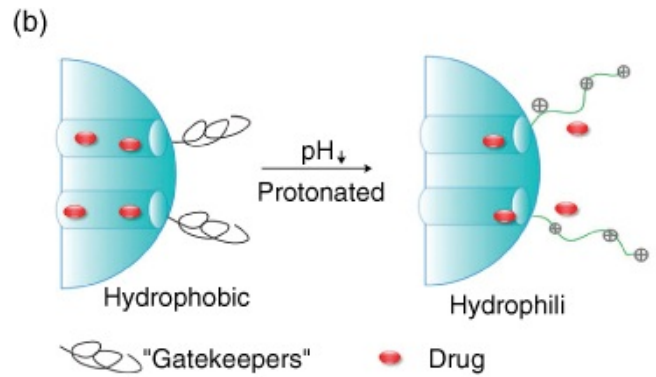
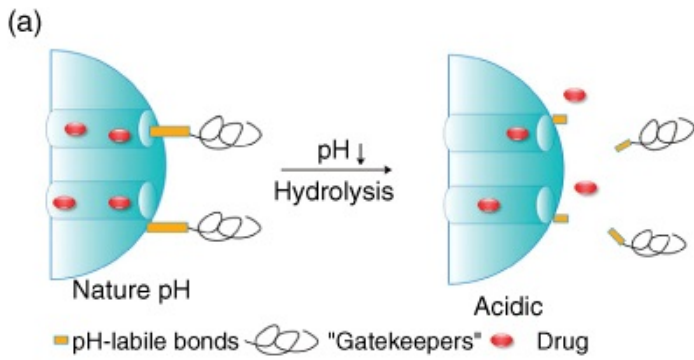


[Figure 5.35](#) Schematic diagram of different stimuli response mechanisms: (a) the first approach for synthesis of a pH-responsive drug delivery system, in which the linker would be cleaved under acidic conditions; (b) another approach for the synthesis of pH-responsive nanocarriers, in which the pKa value of the gatekeeper is near the tumor interstitial pH; (c) a type of charge switching pH-responsive drug delivery system; (d) disulfide-linked drugs or gatekeepers; (e) degradable MSNs; (f) enzyme-sensitive drug delivery vehicles; (g) the light-response mechanism of o-nitrobenzyl, coumarin, and azobenzene; (h) a thermoresponsive drug delivery system.

Source: Reproduced with permission of the RSC [62].

Other pH-sensitive gatekeepers would be acids with a pKa close to the tumor pH. A small change in the pH would protonate multiple sites at the gatekeeper, changing its solubility ([Figure 5.35b](#)). A nice example of this strategy was provided by Bilalis et al. [63]. They capped the drug loaded mesoporous silica particles with poly-L-histidine, with a pKa around 7.0. This closed the pores, until they reach the tumor cells with acidic pH, became protonated, unfolded from the surface and released the drugs.

5.2.3.1 Light Responsive Drug Delivery Systems

Light responsive systems have the advantage that they be controlled from outside, providing that the penetration depth of the laser in the human tissue is deep enough. So near-infrared light is the best option, it has the deepest penetration depth and is less energetic, and thus less damaging to normal tissue.

The classical example was provided by Abe et al. [64]. They used a coumarin modified mesoporous silica ([Figure 5.35g](#)) as a gate keeper. When irradiated at 300–350 nm dimerization of the coumarin occurs. When it is irradiated with light below 260 nm, however, the dimer will dissociate and open the gate. The [Figure 5.35g](#) also reveals that there is still a lot of work ahead of us. The ideal light responsive materials operation at the NIR wavelengths is still not available at this moment.

[Figure 5.35](#) shows many more examples that we cannot discuss within the scope of this book. We refer the reader to the very recent review of Zhu et al. [62] or to one of the many other reviews on this topic. We also refer to the works of Maria Vallet-Regi and coworkers [65].

5.2.4 Low-*k* Dielectrics

Porous silica and organosilicas are very important dielectrical barriers (low-*k* materials) in microelectronic chips. In the continuing miniaturization of electronic devices, manufacturers increase transistor speed, reduce its size, and pack more transistors on a single chip. Nowadays, it is possible to put more than 2 billion transistors on a chip. However, when the interconnecting wires also reduce in size, the resistance of these wires is increased.

$$R = \rho \frac{l}{a}$$

5.8

This phenomenon is described by the relationship in [Eq. 5.8](#), which is known as Pouillet's law and sometimes, incorrectly, referred to as Ohm's law from which it is derived. R is the total resistance, ρ is the material's resistivity, l is the length of the specimen, and a its cross section.

These interconnects come closer together and electrical interference (“cross-talk”) occurs, which is highly undesirable. A very good insulator is required to isolate the different interconnects.

For a long time, this has been normal silica, it has a good mechanical and thermal stability, low leakage current and very high electrical breakdown. However, still RC-delay occurs (resistance capacitance), and better insulators are required.

One pathway is to change the silica insulator ($k = 3.9$) by an insulator with a k -value of 2.2 or below. As dry air is the perfect insulator ($k = 1$) and water is the worst insulator ($k = 80$), a hydrophobic highly porous systems seems ideal. Mesoporous silica films, prepared by the EISA method has gained a lot of attention in this field.

We will discuss the low- k materials in more detail in [Chapter 6](#) on PMOs, as these materials are more promising to reach the targets. We refer you to an excellent review [[66](#)], and to the pioneering papers on this matter by Brinker, Ozin, Landskron, and others.

This was not an exhaustive overview of the applications of mesoporous silica. Applications are in biomedicine, sensing, luminescence, and many others. For a quick overview of some of the most important research in the past decade, we refer you to the reviews in *Chemical Reviews* or *Chemical Society Reviews* [[67](#)].

References

- 1 (a) J. S. Beck, C.-W. Chu, I. Johnson, C. Kresge, M. Leonowicz, W. Roth, J. Vartuli, US Patent, No. US 5098684 1992; (b) Beck, J.S., Vartuli, J.C., Roth, W.J. et al. (1992). *J. Am. Chem. Soc.* 114: 10834–10843; (c) Kresge, C.T., Leonowicz, M.E., Roth, W.J. et al. (1992). *Nature* 359: 710–712.
- 2 Yanagisawa, T., Shimizu, T., Kuroda, K., and Kato, C. (1990). *Bull. Chem. Soc. Jpn.* 63: 988–992.
- 3 Inagaki, S., Fukushima, Y., and Kuroda, K. (1993). *J. Chem. Soc., Chem. Commun.* 680–682.
- 4 Landskron, H., Schmidt, G., Heinz, K. et al. (1991). *Surf. Sci.* 256: 115–122.
- 5 Kresge, C.T. and Roth, W.J. (2013). *Chem. Soc. Rev.* 42: 3663–3670.
- 6 Descalzo, A.B., Martinez-Manez, R., Sancenon, R. et al. (2006). *Angew. Chem. Int. Ed.* 45: 5924–5948.
- 7 (a) Chen, C.-Y., Burkett, S.L., Li, H.-X., and Davis, M.E. (1993). *Microporous Mater.* 2:

- 27–34;(b) Cheng, C.F., He, H.Y., Zhou, W.Z., and Klinowski, J. (1995). *Chem. Phys. Lett.* 244: 117–120.
- 8 Kruk, M., Jaroniec, M., and Sayari, A. (1997). *Langmuir* 13: 6267–6273.
- 9 Ravikovitch, P.I. and Neimark, A.V. (2000). *Langmuir* 16: 2419–2423.
- 10 Huo, Q.S., Margolese, D.I., Ciesla, U. et al. (1994). *Nature* 368: 317–321.
- 11 Tanev, P.T. and Pinnavaia, T.J. (1995). *Science* 267: 865–867.
- 12 Bagshaw, S.A., Prouzet, E., and Pinnavaia, T.J. (1995). *Science* 269: 1242–1244.
- 13 Besson, S., Gacoin, T., Ricolleau, C. et al. (2003). *J. Mater. Chem.* 13: 404–409.
- 14 Huo, Q.S., Leon, R., Petroff, P.M., and Stucky, G.D. (1995). *Science* 268: 1324–1327.
- 15 Van der Voort, P., Mathieu, M., Mees, F., and Vansant, E.F. (1998). *J. Phys. Chem. B* 102: 8847–8851.
- 16 Tanev, P.T. and Pinnavaia, T.J. (1996). *Chem. Mater.* 8: 2068–2079.
- 17 Cassiers, K., Van Der Voort, P., and Vansant, E.F. (2000). *Chem. Commun.* 2489–2490.
- 18 Zhao, D.Y., Sun, J.Y., Li, Q.Z., and Stucky, G.D. (2000). *Chem. Mater.* 12: 275–280.
- 19 Lin, H.P., Tang, C.Y., and Lin, C.Y. (2002). *J. Chin. Chem. Soc.* 49: 981–988.
- 20 Galarneau, A., Nader, M., Guenneau, F. et al. (2007). *J. Phys. Chem. C* 111: 8268–8277.
- 21 Janssen, A.H., Van Der Voort, P., Koster, A.J., and de Jong, K.P. (2002). *Chem. Commun.* 1632–1633.
- 22 Zhao, D.Y., Huo, Q.S., Feng, J.L. et al. (1998). *J. Am. Chem. Soc.* 120: 6024–6036.
- 23 Van Der Voort, P., Ravikovitch, P.I., De Jong, K.P. et al. (2002). *J. Phys. Chem. B* 106: 5873–5877.
- 24 Van Der Voort, P., Ravikovitch, P.I., De Jong, K.P. et al. (2002). *Chem. Commun.* 1010–1011.
- 25 Thommes, M., Kaneko, K., Neimark, A.V. et al. (2015). *Pure Appl. Chem.* 87: 1051–1069.
- 26 Sing, K.S.W., Everett, D.H., Haul, R.A.W. et al. (1985). *Pure Appl. Chem.* 57: 603–619.
- 27 Choi, M., Heo, W., Kleitz, F., and Ryoo, R. (2003). *Chem. Commun.* 1340–1341.
- 28 (a) Zhai, S.R., Park, S.S., Park, M. et al. (2008). *Microporous Mesoporous Mater.* 113: 47–55;(b) Zhai, S.R., Kim, I., and Ha, C.S. (2008). *J. Solid State Chem.* 181: 67–74.

- 29 Guo, W.P., Park, J.Y., Oh, M.O. et al. (2003). *Chem. Mater.* 15: 2295–2298.
- 30 Chen, L.H., Zhu, G.S., Zhang, D.L. et al. (2009). *J. Mater. Chem.* 19: 2013–2017.
- 31 (a) Brinker, C.J., Lu, Y.F., Sellinger, A., and Fan, H.Y. (1999). *Adv. Mater.* 11: 579–585;
(b) Lu, Y.F., Ganguli, R., Drewien, C.A. et al. (1997). *Nature* 389: 364–368.
- 32 Corma, A., Grande, M.S., GonzalezAlfaro, V., and Orchilles, A.V. (1996). *J. Catal.* 159: 375–382.
- 33 van Bekkum, H. and Kloetstra, K.R. (1998). *Stud. Surf. Sci. Catal.* 117: 171–182.
- 34 Tanev, P.T., Chibwe, M., and Pinnavaia, T.J. (1994). *Nature* 368: 321–323.
- 35 Hoffmann, F., Cornelius, M., Morell, J., and Froba, M. (2006). *Angew. Chem. Int. Ed.* 45: 3216–3251.
- 36 Wight, A.P. and Davis, M.E. (2002). *Chem. Rev.* 102: 3589–3613.
- 37 Van Der Voort, P., Baltes, M., and Vansant, E.F. (1999). *J. Phys. Chem. B* 103: 10102–10108.
- 38 (a) Ahonen, M., Pessa, M., and Suntola, T. (1980). *Thin Solid Films* 65: 301–307;(b)
Suntola, T. and Hyvarinen, J. (1985). *Annu. Rev. Mater. Sci.* 15: 177–195.
- 39 Malygin, A.A. (1999). *NATO ASI Ser., Ser. E* 362: 487–495.
- 40 Dendooven, J., Goris, B., Devloo-Casier, K. et al. (2012). *Chem. Mater.* 24: 1992–1994.
- 41 Huang, Y.L., Xu, S., and Lin, V.S.Y. (2011). *Angew. Chem. Int. Ed.* 50: 661–664.
- 42 Zhong, R., Lindhorst, A.C., Groche, F.J., and Kühn, F.E. (2017). *Chem. Rev.* 117: 1970–2058.
- 43 He, Y. and Cai, C. (2011). *Chem. Commun.* 47: 12319–12321.
- 44 Brown, J., Mercier, L., and Pinnavaia, T.J. (1999). *Chem. Commun.* 69–70.
- 45 (a) Snyder, L.R. and Kirkland, J.J. (1979). *Introduction to Modern Liquid Chromatography*, 2e. Wiley;(b) Lembke, P., Henze, G., Cabrera, K. et al. (2008). Liquid chromatography. In: *Handbook of Analytical Techniques* (ed. H. Günzler and A. Williams), 261–326. Wiley-VCH Verlag GmbH.
- 46 Grun, M., Kurganov, A.A., Schacht, S. et al. (1996). *J. Chromatogr. A* 740: 1–9.
- 47 Stober, W., Fink, A., and Bohn, E. (1968). *J. Colloid Interface Sci.* 26: 62–69.
- 48 Destefano, J.J. and Kirkland, J.J. (1974). *J. Chromatogr. Sci.* 12: 337–343.
- 49 Berg, K. and Unger, K. (1971). *Kolloid Z. Z. Polym.* 246: 682.

- 50 Grun, M., Lauer, I., and Unger, K.K. (1997). *Adv. Mater.* 9: 254–257.
- 51 Yang, H., Coombs, N., Dag, O. et al. (1997). *J. Mater. Chem.* 7: 1755–1761.
- 52 Qi, L.M., Ma, J.M., Cheng, H.M., and Zhao, Z.G. (1998). *Chem. Mater.* 10: 1623–1626.
- 53 M. Nyström, W. Herrmann, B. Larsson, Patent, Silica particles, a method for preparation of silica particles and use of the particles, No. EP0298062, 1991.
- 54 Ide, M., Wallaert, E., Van Driessche, I. et al. (2011). *Microporous Mesoporous Mater.* 142: 282–291.
- 55 Martin, T., Galarneau, A., Di Renzo, F. et al. (2004). *Chem. Mater.* 16: 1725–1731.
- 56 Horvath, C. and Lipsky, S.R. (1969). *J. Chromatogr. Sci.* 7: 109.
- 57 Kirkland, J.J. (1969). *Anal. Chem.* 41: 218.
- 58 Kirkland, J.J. (1992). *Anal. Chem.* 64: 1239–1245.
- 59 J. J. Kirkland, T. J. Langlois, US Patent, Process for preparing substrates with a porous surface, No. US2009297853 2009.
- 60 (a) Buchel, G., Unger, K.K., Matsumoto, A., and Tsutsumi, K. (1998). *Adv. Mater.* 10: 1036–1038;(b) J. Glennon, J. Omamogho, International Patent, A process for preparing silica particles, No. WO2010061367 2010.
- 61 T. C. Wei, W. Chen, W. E. Barber, *Polym. Chem.* 2016, 7, 1475–1485.
- 62 Zhu, J.H., Niu, Y.M., Li, Y. et al. (2017). *J. Mater. Chem. B* 5: 1339–1352.
- 63 Bilalis, P., Tziveleka, L.A., Varlas, S., and Iatrou, H. (2016). *Polym. Chem.* 7: 1475–1485.
- 64 Abe, E., Pennycook, S.J., and Tsai, A.P. (2003). *Nature* 421: 347–350.
- 65 (a) Baeza, A., Ruiz-Molina, D., and Vallet-Regi, M. (2017). *Expert Opin. Drug Delivery* 14: 783–796;(b) Castillo, R.R., Baeza, A., and Vallet-Regi, M. (2017). *Biomater. Sci.* 5: 353–377;(c) Castillo, R.R., Colilla, M., and Vallet-Regi, M. (2017). *Expert Opin. Drug Delivery* 14: 229–243;(d) Doadrio, A.L., Salinas, A.J., Sanchez-Montero, J.M., and Vallet-Regi, M. (2015). *Curr. Pharm. Des.* 21: 6189–6213;(e) Martinez-Carmona, M., Colilla, M., and Vallet-Regi, M. (2015). *Nanomaterials* 5: 1906–1937;(f) Vallet-Regi, M. (2006). *Chem. Eur. J.* 12: 5934–5943;(g) Vallet-Regi, M. (2010). *J. Intern. Med.* 267: 22–43;(h) Vallet-Regi, M., Balas, F., Colilla, M., and Manzano, M. (2007). *Solid State Sci.* 9: 768–776;(i) Vallet-Regi, M., Colilla, M., and Gonzalez, B. (2011). *Chem. Soc. Rev.* 40: 596–607;(j) Vallet-Regi, M.A., Ruiz-Gonzalez, L., Izquierdo-Barba, I., and Gonzalez-Calbet, J.M. (2006). *J. Mater. Chem.* 16: 26–31.
- 66 Lioni, K., Volksen, W., Magbitang, T. et al. (2015). *ECS J. Solid State Sci. Technol.* 4: N3071–N3083.

67 (a) Chaudhuri, R.G. and Paria, S. (2012). *Chem. Rev.* 112: 2373–2433;(b) Ciriminna, R., Fidalgo, A., Pandarus, V. et al. (2013). *Chem. Rev.* 113: 6592–6620;(c) Valtchev, V. and Tosheva, L. (2013). *Chem. Rev.* 113: 6734–6760;(d) Deng, Y.H., Wei, J., Sun, Z.K., and Zhao, D.Y. (2013). *Chem. Soc. Rev.* 42: 4054–4070;(e) Han, W.S., Lee, H.Y., Jung, S.H. et al. (2009). *Chem. Soc. Rev.* 38: 1904–1915;(f) Innocenzi, P. and Malfatti, L. (2013). *Chem. Soc. Rev.* 42: 4198–4216;(g) Li, Z.X., Barnes, J.C., Bosoy, A. et al. (2012). *Chem. Soc. Rev.* 41: 2590–2605;(h) Parlett, C.M.A., Wilson, K., and Lee, A.F. (2013). *Chem. Soc. Rev.* 42: 3876–3893;(i) Perego, C. and Millini, R. (2013). *Chem. Soc. Rev.* 42: 3956–3976;(j) Qiu, H.B. and Che, S.N. (2011). *Chem. Soc. Rev.* 40: 1259–1268;(k) Wagner, T., Haffer, S., Weinberger, C. et al. (2013). *Chem. Soc. Rev.* 42: 4036–4053;(l) Walcarius, A. (2013). *Chem. Soc. Rev.* 42: 4098–4140;(m) Wen, J., Yang, K., Liu, F.Y. et al. (2017). *Chem. Soc. Rev.* 46: 6024–6045;(n) Wu, S.H., Mou, C.Y., and Lin, H.P. (2013). *Chem. Soc. Rev.* 42: 3862–3875;(o) Yang, P.P., Gai, S.L., and Lin, J. (2012). *Chem. Soc. Rev.* 41: 3679–3698;(p) Zaera, F. (2013). *Chem. Soc. Rev.* 42: 2746–2762.

Note

$D_{90/10}$ is a statistic describing the dispersion on the particle size. D_{10} is the particle diameter where the cumulative volume of the particles reaches 10%. D_{90} is the corresponding value at 90 v%.